PHYSICAL REVIEW C VOLUME 26, NUMBER 2 AUGUST 1982

Multistep direct reaction analysis of continuum spectra in reactions induced by light ions

T. Tamura, T. Udagawa, and H. Lenske
Department of Physics, University of Texas, Austin, Texas 78712
(Received 11 March 1982)

Analyses of continuum spectra of light-ion reactions, in terms of multistep direct reaction methods are discussed. The formulation used in the calculations is presented first, and is followed by several examples which show that this method works rather well in a variety of cases. Comparison with related theories is also made.

[NUCLEAR REACTIONS Multistep direct reaction method, calculations of cross sections, and polarizations of continuum spectra of reactions induced by light ions.]

I. INTRODUCTION

During the past two decades, the direct reaction (DR) method has been used extensively and successfully in analyzing a large amount of experimental data for nuclear reactions induced both by light and heavy ions. As is well known, the simplest version of the DR method is the distorted wave Born approximation (DWBA).[1,2] With the purpose of analyzing data that involve contributions of more complicated (multistep) processes, techniques like the coupled-channels Born approximation (CCBA) (Refs. 2 and 3) and coupled-reaction-channels (CRC) (Refs. 4 and 5) methods were also developed. With emphasis on the "multistep" aspects, we may refer to all these methods (including DWBA) as the multistep direct reaction (MSDR) method.

Past applications of the MSDR method have been limited to processes in which the members of the pair of residual nuclei were left in their respective discrete states, i.e., processes which we may refer to as "discrete state transitions." The purpose of the present paper is to show that the MSDR method can be extended to reactions in which one of the residual nuclei is left in its continuum states, i.e., processes which we may refer to as "continuum transitions." In several recent publications, we have in fact demonstrated that it was possible, with this MSDR approach, to fit a variety of continuum transition data observed in reactions induced by both light and heavy ions.

In the present paper, we shall concentrate on light-ion induced reactions. Since our earlier publications related to this subject[6–14] were all short, presenting various materials in a somewhat fragmentary way, we intend to make here a much better organized presentation of these materials. The reader who is interested in the heavy-ion counterpart of the material given in the present paper is referred to recent review articles.[15]

The basic justification for use of the MSDR method in continuum transitions is presented in Sec. II. As will be seen, the key is a statistical consideration. In continuum transitions, a large number of very complicated eigenstates are involved, and to calculate cross sections to excite these states individually is impracticable. However, a statistical argument shows that the *sum* of these cross sections, which is our only interest, can be replaced by another *sum* of cross sections exciting a much smaller number of much simpler states. The MSDR method is very appropriate to calculate the latter type of cross sections.

In Sec. III, we recapitulate the derivation of the MSDR cross sections, in spite of the fact that it is a very well known subject. This is because we intend to present the various quantities concretely and precisely, so that, e.g., approximations which we introduce later (Sec. IV) can be understood unambiguously. As will be seen, we start Sec. III with the CRC equations, but are satisfied with solving them perturbatively, thus obtaining the Born series. Therefore, the MSDR method in the present paper is, in fact, a higher order (including the first order) DWBA.

In Sec. IV, we derive the expressions for the continuum cross sections by combining the DWBA cross sections of Sec. III with the spectroscopic den-

sities, the latter describing the statistical and the nuclear structure aspects involved in the reaction. In both Secs. III and IV, we present the various expressions only up to the second order terms. We believe, however, that the reader will find it easy to figure out, from what we have given, how to extend the formalism to still higher orders, if such become necessary. In Sec. V, we present a few examples of actual calculations made by using the formulas given in Secs. III and IV, and compare them with experimental data. It is seen that the fits to data we achieve are very good, in general. In Sec. VI, we discuss related works by other authors, and in Sec. VII, we summarize the present paper.

II. STATISTICAL AND NONSTATISTICAL ASPECTS IN THE FORMULATION OF THE MSDR CONTINUUM CROSS SECTIONS

To make the presentation clear, let us begin by restricting ourselves to the (p,p') reactions. We also assume that the target is in a doubly-closed-shell configuration, and that the residual interaction that causes the inelastic scattering is of a two-body nature. Then the one-step processes will proceed by creating 1p-1h (one-particle–one-hole) states, two-step processes 2p-2h states, and so forth. We may call these np-nh states ($n=1,2,\ldots$) elementary (or basis) states.

Even when the target is legitimately assumed to have a purely doubly-closed-shell configuration, it is reasonable to expect that each excited eigenstate $|n\rangle$ (with an eigenenergy E_n) is given as a complicated linear combination of elementary states. Having in mind the description of one-step processes first, we may write this state as

$$|n\rangle=\sum_B a_B^{(n)}|B\rangle+\delta|n\rangle\ . \tag{2.1}$$

Here, we denote by $|B\rangle$ a 1p-1h state, and by $\delta|n\rangle$ a sum of more complicated elementary states. The (one-step) DWBA amplitude $T_n^{(1)}$ to excite this state may then be written as

$$T_n^{(1)}=\langle\chi_b|\langle n|v|0\rangle|\chi_a\rangle=\sum_B a_B^{(n)}t_{ba}^B\ , \tag{2.2a}$$

with

$$t_{ba}^B=\langle\chi_b|v_{B0}|\chi_a\rangle;\quad v_{B0}=\langle B|v|0\rangle\ . \tag{2.2b}$$

In (2.2), we denoted by $|0\rangle$ the ground state wave function of the target, and by $|\chi_a\rangle$ and $|\chi_b\rangle$ the distorted waves in the incident and exit channels, respectively. Clearly, $\delta|n\rangle$ of (2.1) does not contribute to (2.2). We also note here that it is very reasonable to assume that the amplitudes $a_B^{(n)}$ are random, in both sign and magnitude.

In the continuum region, there will be contained a large number of eigenstates, even when a relatively narrow energy interval is taken. The measured cross section is then a sum of cross sections exciting these eigenstates. More precisely, the experimental spectrum of the cross sections, i.e., the continuum cross section per unit energy, should be interpreted as an energy average of the sum of cross sections taken over a large number of these states.

Using the transition applitude $T_n^{(1)}$ given by (2.2a), we can write the energy averaged one-step cross section as

$$\begin{aligned}\frac{d^2\sigma^{(1)}(E_p')}{dE_p'd\Omega_p}&=\sum_n|T_n^{(1)}|^2\delta(E_n-E_x)\\&=\sum_n\delta(E_n-E_x)\\&\quad\times\sum_{BB'}a_B^{(n)}a_{B'}^{(n)}t_{ba}^Bt_{ba}^{B'*}\\&=\sum_B c_B(E_x)|t_{ba}^B|^2\\&=\sum_B c_B(E_x)d\sigma_B^{(1)}(E_p')/d\Omega_p\ .\end{aligned} \tag{2.3}$$

The δ function appearing in the first and second lines of (2.3) restricts the sum over those $|n\rangle$'s whose eigenenergies E_n agree with the excitation energy E_x, which in turn satisfies a relation that $E_x=E_p-E_{p'}$, where E_p and $E_{p'}$ are, respectively, the proton energies in the incident and exit channels. As is well known, to take the sum over n, with the δ function in it this way, is equivalent to calculating the energy averaged sum. In fact, one may first take a sum over the states $|n\rangle$ within a certain energy interval ΔE, centered at E_x, and then divide the sum by ΔE. One then sees that a sum over n, including $\delta(E_n-E_x)$ in the summand, emerges.

In obtaining the third equality of (2.3), we used the relation that

$$\sum_n a_B^{(n)}a_{B'}^{(n)}\delta(E_n-E_x)=\delta_{BB'}c_B(E_x)\ . \tag{2.4a}$$

This relation is a direct consequence of our assumption, made above, that $a_B^{(n)}$'s are random, which

makes $a_B^{(n)}a_{B'}^{(n)}$ also random, both in sign and magnitude, except that randomness in sign is not the case if $B=B'$. The appearance of $\delta_{BB'}$ in (2.4a) is thus understood. If it were not for the δ function, Eq. (2.4a) would be nothing but the completeness relation, and we should have had simply $\delta_{BB'}$ on the rhs. The presence of the δ function, however, restricts the sum to those $|n\rangle$'s that lie within a unit energy interval, and thus an additional factor $c_B(E_x)<1$ appears.

Equation (2.4a) permits us to express $c_B(E_x)$ as

$$c_B(E_x)=da_B{}^2(E_x)/dE_x \ . \tag{2.4b}$$

Therefore, it is very reasonable to interpret $c_B(E_x)$ as the probability (per unit energy), that the state $|B\rangle$ is located at the excitation energy E_x. In practice, one may take, e.g., a Gaussian or a Lorentzian form for $c_B(E_x)$, with a width Γ, and centered at E_B, the unperturbed energy of $|B\rangle$;

$$c_B(E_x)=\exp[-(E_x-E_B)^2/\Gamma^2]/(\sqrt{\pi}\Gamma) \ , \tag{2.4c}$$

or

$$c_B(E_x)=(\Gamma/\pi)[(E_x-E_B)^2+\Gamma^2]^{-1} \ . \tag{2.4d}$$

The last equality of (2.3) defines the DWBA cross section exciting an elementary state $|B\rangle$ located at E_x as

$$d\sigma_B^{(1)}(E_p')/d\Omega_p=|t_{ba}^B|^2 \ .$$

[A constant factor that might have appeared in this equation and also in (2.3) was suppressed for simplicity.] A standard DWBA technique, as will be described in Sec. III, may be used to evaluate $d\sigma_B^{(1)}/d\Omega_p$. Combining this with the $c_B(E_x)$ factor discussed above, it is straightforward to evaluate the last expression of (2.3), and thus the one-step contributions $d^2\sigma^{(1)}/dE_p'd\Omega_p$ to the continuum (p,p') cross sections.

We shall now proceed to formulate the two-step cross sections. We denote the final state again by $|n\rangle$, and an eigenstate excited by the first of the two steps by $|n'\rangle$. The second order DWBA amplitude describing this two-step process may then be written as

$$T_n^{(2)}=\sum_{n'}\langle\chi_b|\langle n|v|n'\rangle|\chi_c\rangle \times G_c\langle\chi_c|\langle n'|v|0\rangle|\chi_a\rangle \ . \tag{2.5}$$

We summed over n', because many intermediate states $|n'\rangle$ can contribute coherently to the above type of two-step processes, and the amplitudes corresponding to different $|n'\rangle$'s do interfere with each other. We shall show shortly, however, that this interference disappears because of the statistical nature of the expansion coefficients appearing in the final states; cf. (2.7).

In (2.5) $|n'\rangle$ appears twice, once as $|n'\rangle$ in the first matrix element, and then as $\langle n'|$ in the second matrix element. In the latter appearance, we may treat it in the same way as we treated $\langle n|$ for the one-step transition in (2.2), and obtain

$$\langle\chi_c|\langle n'|v|0\rangle|\chi_a\rangle=\sum_C a_C^{(n')}t_{ca}^C \ . \tag{2.6}$$

Again a term in $\langle n'|$ which might have been written as $\delta\langle n'|$ did not contribute (2.6). However, to ignore $\delta|n'\rangle$ in $|n'\rangle$ that appears in the first matrix element of (2.5) is erroneous. This is because the state $\langle n'|$ is created *as a whole* by the first step, despite the fact that only its small portion $\sum_C a_C^{(n')}\langle C|$ is utilized for its excitation.

We shall thus leave $|n'\rangle$ just as it stands, without expanding it in terms of elementary states. On the other hand, we may write $|n\rangle$ as

$$|n\rangle=\sum_{Bn''}a_{Bn''}^{(n)}|B,n''\rangle+\delta|n\rangle \ . \tag{2.7}$$

Clearly, the first term of (2.7) is a sum of states which are constructed by adding a (new) 1p-1h pair B to eigenstates $|n''\rangle$, and $\delta|n\rangle$ includes those that are not written in the form of the first term.

By using (2.7), we may evaluate $\langle n|v|n'\rangle$ as

$$\langle n|v|n'\rangle=\sum_{Bn''}a_{Bn''}^{(n)}\langle B,n''|v|n'\rangle =\sum_B a_{Bn'}^{(n)}v_{B0} \ , \tag{2.8}$$

where we used the assumption that

$$\langle B,n''|v|n'\rangle=\langle B|v|0\rangle\delta_{n'n''}=v_{B0}\delta_{n'n''} \ . \tag{2.9}$$

What underlies (2.9) is a view that a (p,p') step always proceeds by creating a new *ph* pair, and thus that the (large number of) *ph* pairs that might have been present in $|n'\rangle$ play only the role of a spectator, thus resulting in $\delta_{n'n''}$. To assume this spectator nature is the same as to neglect in the (p,p') step the so-called *scattering processes,* in which a particle (or a hole) is scattered from one orbit into another. Since the statistical weight of such a scattering process is much smaller than is that of pair creation

processes, to neglect the former processes, and thus to make the spectator assumption, is very much in line with the other statistical assumptions we are making.

If we use (2.6) and (2.8), then $T_n^{(2)}$ of (2.5) is rewritten as

$$T_n^{(2)}=\sum_{n'}\sum_{BC} a_{Bn}^{(n)}a_C^{(n')}t_{bca}^{BC}\ ;$$

$$t_{bca}^{BC}=t_{bc}^{B}G_c t_{ca}^{C}\ . \tag{2.10}$$

The two-step contribution to the continuum cross section is then given as

$$\frac{d^2\sigma^{(2)}(E_p',E_p'')}{dE_p'\,d\Omega_p}=\sum_n |\,T_n^{(2)}\,|^2\delta(E_n-E_x)$$

$$=\sum_n \delta(E_n-E_x)\sum_{BB'CC'}\sum_{n'n''} a_{Bn'}^{(n)}a_{B'n''}^{(n)}a_C^{(n')}a_C^{(n'')}t_{bca}^{BC}t_{bca}^{BC'*}\ . \tag{2.11}$$

Here again, $E_x=E_p-E_p'$, the meaning of E_p and E_p' being also the same as before. On the other hand, E_p'' is the energy of the proton in the asymptotic region in the intermediate channel. By using (2.4a), and also a relation that

$$\sum_n a_{Bn'}^{(n)}a_{B'n''}^{(n)}\delta(E_n-E_x)=\delta_{BB'}\delta_{n'n''}c_{Bn'}(E_x)\ , \tag{2.12}$$

which is similar to (2.4a), and is derived by using again the random sign hypothesis of the coefficients $a_{Bn'}^{(n)}$, the rhs of (2.11) can be calculated as follows:

$$\text{rhs of (2.11)}=\sum_B\sum_{CC'}\sum_{n'} c_{Bn'}(E_x)a_C^{(n')}a_{C'}^{(n')}t_{bca}^{BC}t_{bca}^{BC'*}$$

$$=\sum_B\sum_{CC'}\int dE_x'\sum_{n'}\delta(E_n'-E_x')a_C^{(n')}a_{C'}^{(n')}c_{Bn'}(E_x)t_{bca}^{BC}t_{bca}^{BC'*}$$

$$=\sum_{BC}\int dE_x' c_C(E_x')c_B(E_x'')\,|\,t_{bca}^{BC}\,|^2\ . \tag{2.13}$$

Here $E_x'=E_p-E_p''$ and $E_x''=E_p''-E_p'$, which are, respectively, the energies transferred to the target during the first and the second step processes. In going from the second to third line in (2.13), we made an approximation that

$$c_{Bn'}(E_x)=c_{Bn'}(E_x''+E_x')\simeq c_B(E_x'')\ . \tag{2.14}$$

It is easy to see that the assumption made in (2.14) is nothing but the spectator nature of the (preformed) *ph* pairs in $|\,n'\rangle$, the same assumption that was made in obtaining Eq. (2.9) above. More precisely, we assumed in (2.14) that the (relative) probability with which a new *ph* pair B is created is the same, irrespective of whether it is created in a complicated state $|\,n'\rangle$, or in the (simple) ground state $|\,0\rangle$, so long as the energy E_x'' associated with its creation is the same.

If we further define

$$d\sigma_{BC}^{(2)}(E_p',E_p'')/d\Omega_p$$

by

$$d\sigma_{BC}^{(2)}(E_p',E_p'')/d\Omega_p=|\,t_{bca}^{BC}\,|^2\ , \tag{2.15}$$

and also change the integration variable in (2.13) from E_x' to E_p'', we finally obtain

$$d^2\sigma^{(2)}(E_p')/dE_p'\,d\Omega_p=\sum_{BC}\int_{E_p'}^{E_p} c_B(E_p''-E_p')c_C(E_p-E_p'')[d\sigma_{BC}^{(2)}(E_p',E_p'')/d\Omega_p]\,dE_p''\ . \tag{2.16}$$

The upper and lower limits of the above integral are seen to guarantee that the arguments of the $c_B(E_x)$ factors remain non-negative. This is the consequence of our treatment that each step proceeds by *creating* a *ph* pair, i.e., by exciting the target. Deexcitation of the target never takes place in our treatment, which neglects the scattering processes, as explained above.

It is remarkable that the cross sections (2.3) and (2.16) are obtained as sums over cross sections creating elementary states, thus making the actual calculations practicable. The absence of the in-

terference between amplitudes creating different elementary states is, of course, due to the use of the statistical assumptions, which resulted in Kronecker delta factors like $\delta_{BB'}$ and $\delta_{CC'}$. We shall now show that, within the same statistical assumption, the interference between the one- and two-step amplitudes also disappears.

Let us denote by $\sigma^{(1,2)}$ the possible contribution of this interference to the continuum cross section. It may be expressed as

$$\begin{aligned}\sigma^{(1,2)}&=\sum_n T_n^{(1)*}T_n^{(2)}\delta(E_n-E_x)+\text{c.c.}\\&=\sum_n\delta(E_n-E_x)\left[\sum_{B'}a_{B'}^{(n)}t_{ba}^{B'*}\right]\left[\sum_{n'BC}a_{Bn'}^{(n)}a_C^{(n')}t_{bca}^{BC}\right]+\text{c.c.}\\&=\sum_{BB'Cn'}\left[\sum_n a_{B'}^{(n)}a_{Bn'}^{(n)}\delta(E_n-E_x)\right]a_C^{(n')}\{t_{ba}^{B'*}t_{bca}^{BC}+\text{c.c.}\}\ .\end{aligned}\tag{2.17}$$

In the last line of (2.17) we may perform the summation over n first, which results in a factor $\delta_{BB'}\delta_{n'0}$. The second Kronecker delta $\delta_{n'0}$, which originates from the fact that $a_B^{(n)}$ could also have been written as $a_{B0}^{(n)}$, makes the summand of the last line of (2.17) proportional to $a_C^{(0)}$. Since $a_C^{(0)}=0$, because a vacuum cannot contain a *ph* pair, we obtain $\sigma^{(1,2)}=0$.

The significance of the results (2.3) and (2.16) is that they show that, for our purpose, the elementary states can be treated as if they were eigenstates, in spite of the fact that their amplitudes are distributed over a large number of very complicated nuclear eigenstates. Once seen from this point of view, the absence of the interference between one- and two-step amplitudes is obvious. They are amplitudes exciting different eigenstates.

Since we have explained in detail the derivation of the one- and two-step continuum cross sections, it will be easy to see what the continuum cross sections corresponding to still higher order steps would look like. It will also be easy to see that results like (2.3) and (2.16) can also be used to describe cross sections for reactions other than (p,p'), by appropriately reinterpreting the various quantities that appear in these expressions. Consider, for example, a (p,α) reaction. In (2.3), the state $|B\rangle$ may then be interpreted to mean a three-hole ($3h$) state, and $\sigma_B^{(1)}(E_\alpha)/d\Omega_\alpha$ a DWBA cross section of this (p,α) process.

In Sec. III, we discuss calculations of the elementary DWBA cross sections $d\sigma^{(1)}/d\Omega_p$ and $d\sigma^{(2)}/d\Omega_p$, while the use of the function $c_B(E)$ will be discussed in Sec. IV, in combination with the spectroscopic factor which is to be introduced in Sec. III.

III. DWBA CROSS SECTIONS

The derivation of the DWBA cross sections, not only of the first order, but also of the higher orders, is well known.[1–5] We nevertheless present it here, so that this paper becomes self-contained. We intend to make the presentation as compact as possible. We formulate the calculation for an even-even target, with $I_A=M_A=0$. The result may nevertheless be used also for odd-A and odd-odd targets because, for our present purpose, the extra nucleons (or holes) outside the even-even core may very well be treated as spectators.

A. The CRC equation

The total wave function of the system may be written as

$$\psi^{(+)}=\sum_{\beta,\alpha}r^{-1}\chi_{\beta,\alpha}(r_b)\,|\beta\rangle\ .\tag{3.1}$$

Here $\chi_{\beta,\alpha}(r_b)$ denotes the (radial part of the) distorted wave in the channel β, obtained with the condition that the incident wave is present only in the channel α. Further in (3.1), $|\beta\rangle$ is the channel wave function which we may write as

$$|\beta\rangle=|l_bs_bj_bq_b\rangle\,|I_BM_B\rangle\ ,\tag{3.2a}$$

with

$$|l_bs_bj_bq_b\rangle=\sum_{m_bn_b}(l_bm_bs_bn_b\,|\,j_bq_b)\times i^{l_b}Y_{l_bm_b}\xi_{s_bn_b}\ ,\tag{3.2b}$$

where $(l_bm_bs_bn_b\,|\,j_bq_b)$ is the Clebsch-Gordan coefficient, while Y_{lm} and ξ_{sn} are, respectively, the spherical harmonics (with the Condon-Shortley phase) and the intrinsic wave function of the projectile. $|I_BM_B\rangle$ is the target (or the residual nucleus) wave function. We also remark here that, in the following, we sometimes use b to mean a pair of quantum numbers l_b and j_b. Thus, e.g., $\sum_b$ means a sum over partial waves in the channel β.

The equation for the radial (distorted wave) function $\chi_{\beta,\alpha}$ may be derived by inserting (3.1) into the Schrödinger equation for the total system, and then projecting out the β channel component. In doing this, we introduce two approximations; the zero-range approximation, and neglect of the nonorthogonality terms. The resultant equation then reads[5]

$$D_b(r_b)\chi_{\beta,\alpha}(r_b)=\Sigma_\gamma v_{\beta,\gamma}(r_c)\chi_{\gamma,\alpha}(r_c)\ , \tag{3.3a}$$

where

$$v_{\beta,\gamma}\equiv\langle\beta\,|\,V\,|\,\gamma\rangle \tag{3.3b}$$

and

$$D_b(r_b)=\left[\frac{\hbar^2}{2\mu_b}\right]\left\{\frac{d^2}{dr_b{}^2}-\frac{l_b(l_b+1)}{r_b{}^2}\right\} -U_b(r_b)+E_b\ . \tag{3.3c}$$

With the zero-range approximation, the coordinate r_b in channel β is very conveniently written as[5] $r_b=(A/B)r$, where A is the target mass and B is the mass of the residual nucleus in the channel β. This relation is true for all the channels, and thus we have, e.g., $r_c=(A/C)r$. We further have $r_a=r$. The above rule thus offers a very convenient way to *rescale* coordinates in different channels, once an appropriate scaling is introduced in the incident channel α. In Eq. (3.3c), μ_b, U_b, and E_b are, respectively, the reduced mass, the optical potential, and the kinetic energy of the relative motion, all in the channel β.

The interaction matrix element $v_{\beta,\gamma}$, defined by (3.3b), can in general be cast into the following form

$$v_{\beta,\gamma}(r_c)=\sum_J d_J^{BC}F_J^{BC}(r_c)B_J(b,c) \times(I_CM_Cjm_j\,|\,I_BM_B) \times(-)^{j_b-q_b}(j_cq_cj_b-q_b\,|\,jm_j)\ . \tag{3.4a}$$

Here $F_J^{BC}(r_c)$ is defined as

$$F_J^{BC}(r_c)=(B/C)^2f_J^{BC}(r_c)\ , \tag{3.4b}$$

where $f_J^{BC}(r_c)$ is the function, which is conventionally called the form factor. To be noted, nevertheless, is the fact that its argument must be r_c, rather than r_b or the simple r $(=r_a)$. Keep in mind that we are considering here a transition from the channel γ to β. The appearance of this r_c, and that of the extra factor $(B/C)^2$ in (3.4b), is the result of our systematic choice of the different scaling of coordinates in different channels, as explained above.

The index J, that appeared in (3.4a) and (3.4b), stands for a set of quantum numbers, l, s, and j, which are, respectively, the transferred orbital, spin, and the total angular momenta; $J=\{l,s,j\}$. In (3.4a)

$$B_J(b,c)=A_{l_bl_cl}\hat{j}_b\hat{j}_c\hat{l}\hat{s}\begin{Bmatrix} l_c & s_c & j_c \\ l_b & s_b & j_b \\ l & s & j \end{Bmatrix}\ ; \qquad [\hat{j}=(2j+1)^{1/2}]\ , \tag{3.4c}$$

with

$$A_{l_bl_cl}=[4\pi]^{-1/2}\hat{l}_b\hat{l}_c\hat{l}^{-1}i^{l_b+l_c-l} \times(l_c0l_b0\,|\,l0)\ . \tag{3.4d}$$

Finally, d_J^{BC}, also in (3.4a), is the spectroscopic amplitude, which will be discussed in detail in Sec. IV, together with the form factor $F_J(r)$.

B. Perturbative solutions

In the MSDR calculations of the present paper, we obtain the distorted wave $\chi_{\alpha,\beta}$ by expanding it in the sense of the Born approximation, i.e., as

$$\chi_{\beta\alpha}=\delta_{\beta\alpha}\chi_\alpha^{(0)}+\chi_{\beta,\alpha}^{(1)}+\chi_{\beta,\alpha}^{(2)}+\cdots\ . \tag{3.5}$$

The behavior in the β channel in the ith step is described by the ith term in (3.5). These terms are to be obtained as solutions of a chain of equations, the first three of which being given by

$$D_a(r)\chi_\alpha^{(0)}(r)=0\ , \tag{3.6a}$$

$$D_b(r_b)\chi_{\beta,\alpha}^{(1)}(r_b)=v_{\beta,\alpha}(r)\chi_\alpha^{(0)}(r)\ , \tag{3.6b}$$

$$D_b(r_b)\chi_{\beta,\alpha}^{(2)}(r_b)=\Sigma_\gamma v_{\beta,\gamma}(r_c)\chi_{\gamma,\alpha}^{(1)}(r_c)\ . \tag{3.6c}$$

Equation (3.6a), for the usual optical model wave function $\chi_\alpha^{(0)}$, is to be solved with the asymptotic condition that

$$\chi_\alpha^{(0)}\underset{r\to\infty}{\longrightarrow}\exp[i\sigma_{l_a}]\{F_{l_a}+C_aH_{l_a}^{(+)}\}\ , \tag{3.7}$$

where F_l and $H_l^{(+)}$ are, respectively, the regular and the outgoing Hankel Coulomb wave functions, while σ_{l_a} is the Coulomb phase shift.

Instead of solving (3.6b) and (3.6c) as they stand, it is convenient to decompose first $\chi_{\beta,\alpha}^{(1)}$ and $\chi_{\beta,\alpha}^{(2)}$ as

$$\chi^{(1)}_{\beta,\alpha}=\sum_J d_J^{BA}B_J(b,a)(a\tilde{b}\,|\,j)\chi^{(1)BA}_{Jb,a}\ , \tag{3.8a}$$

$$\chi^{(2)}_{\beta,\alpha}=\sum_C\sum_{J_1J_2Jc} d_{J_2J_1}^{BC_dCA}B_{J_2}(b,c)B_{J_1}(c,a)(-)^{j_1+j_2-j}W(j_aj_bj_1j_2;jj_c)(a\tilde{b}\,|\,j)\chi^{(2)BCA}_{J_2b,J_1c,a}\ , \tag{3.8b}$$

where

$$(a\tilde{b}\,|\,j)\equiv(j_aq_aj_b\tilde{q}_b\,|\,jm_j)$$
$$=(-)^{j_b-q_b}(j_aq_aj_b-q_b\,|\,jm)\ .$$

In writing (3.8), we have already used the fact that we chose $I_A=M_A=0$, which makes $I_B=j$ and $M_B=m_j$, where j is the total angular momentum transferred (see above), and m_j is its projection. Note that, as was seen in (3.6), we denote the final channel always by β. In (3.8b) we have $\vec{j}=\vec{j}_1+\vec{j}_2$, where j_1 (j_2) is the total angular momentum transferred in the first (second) step, which goes from the channel α (γ) to the channel γ (β). It should also be noted that (3.8b) involves a sum over C, the intermediate states, and that over c, the partial waves in the corresponding intermediate channel.

We solve the set of equations

$$D_b(r_b)\chi^{(1)BA}_{J_1b,a}(r_b)=F^{BA}_{J_1}(r)\chi^{(0)}_a(r)\ , \tag{3.9a}$$

$$D_b(r_b)\chi^{(2)BCA}_{J_2b,J_1c,a}(r_b)=F^{BC}_{J_2}(r_c)\chi^{(1)CA}_{J_1c,a}(r_c)\ , \tag{3.9b}$$

with the asymptotic condition that

$$\chi^{(1)BA}_{J_1b,a}\underset{r\to\infty}{\to}\exp(-i\sigma_{l_b})C^{(1)BA_H(+)}_{J_1b,al_b}\ , \tag{3.10a}$$

$$\chi^{(2)BCA}_{J_2b,J_1c,a}\underset{r\to\infty}{\to}\exp(-i\sigma_{l_b})C^{(2)BCA}_{J_2b,J_1c,a}H^{(+)}_{l_b}\ . \tag{3.10b}$$

Let us define $X^{(1)BA}_{Jb,a}$ and $X^{(2)BCA}_{Jb,a}$ by

$$X^{(1)BA}_{Jb,a}=d_J^{BA}B_J(b,a)C^{(1)BA}_{Jb,a}\ , \tag{3.11a}$$

$$X^{(2)BCA}_{Jb,a}=\sum_{J_1J_2c} d_{J_2}^{BC}d_{J_1}^{CA}B_{J_2}(b,c)B_{J_1}(c,a)(-)^{j_1+j_2-j}\hat{j}_1\hat{j}_2W(j_aj_bj_1j_2;jj_c)C^{(2)BCA}_{J_2b,J_1c,a}\ . \tag{3.11b}$$

We then have obviously

$$\chi^{(1)}_{\beta,\alpha}\underset{r\to\infty}{\to}\sum_J X^{(1)BA}_{Jb,a}(a\tilde{b}\,|\,j)[\exp(-i\sigma_{l_b})H^{(+)}_{l_b}]\ , \tag{3.12a}$$

$$\chi^{(2)}_{\beta,\alpha}\underset{r\to\infty}{\to}\sum_{J,C} X^{(2)BCA}_{Jb,a}(a\tilde{b}\,|\,j)[\exp(-i\sigma_{l_b})H^{(+)}_{l_b}]\ . \tag{3.12b}$$

C. Transition amplitudes and cross sections

The transition amplitude, from the initial channel α to the final channel β, may most generally be written as $T_{s_bn_bI_BM_B,s_an_aI_AM_A}$. Since, however, we have decided to always choose $I_A=M_A=0$, which makes $I_B=j$ and $M_B=m_j$, we may use a somewhat simplified form for it; $T_{s_bn_bjm_j;s_an_a}$. This amplitude is defined so that the asymptotic form of the total wave function is written as

$$\Psi^{(+)}\to\sum_{l_a}(1/r)\hat{l}_a\exp(i\sigma_{l_a})F_{l_a}\,|\,l_a0s_an_a\rangle\,|\,00\rangle$$
$$+\sum_\beta[k_a^2v_a/(4\pi v_b)]^{1/2}T_{s_bn_bjm_j;s_an_a}\left\{\frac{1}{r}\exp(-i\sigma_{l_b})i^{l_b}H^{(+)}_{l_b}\right\}$$
$$\times\,|\,l_bm_bs_bn_b\rangle\,|\,I_BM_B\rangle\ . \tag{3.13}$$

Here, e.g., $|\,l_bm_bs_bn_b\rangle=i^{l_b}Y_{l_bm_b}\xi_{s_bn_b}$. Compare with Eq. (3.2b).

Corresponding to the expansion of $\chi_{\beta,\alpha}$ as done in (3.5), it is convenient to expand the above transition amplitude as

$$T_{s_b n_b j m_j; s_a n_a} = \sum_{i=1}^{\infty} T^{(i)}_{s_b n_b j m_j; s_a n_a} \ . \tag{3.14}$$

We may make $r \to \infty$ in (3.1), in which $\chi_{\beta,\alpha}$ is expanded as in (3.5), so that the asymptotic form of (3.12) can be used. If we compare the resultant form with (3.13), combined with (3.14), we easily find that

$$T^{(1);B}_{s_b n_b j m_j; s_a n_a}(\theta_b,\phi_b) = \sum_{J,ab} g^{(a,b)}_{s_b n_b s_a n_a; j m_j}(\theta_b \phi_b) X^{(1)BA}_{Jb;a} \ , \tag{3.15a}$$

$$T^{(2);BC}_{s_b n_b j m_j; s_a n_a}(\theta_b,\phi_b) = \sum_{J,Cab} g^{(a,b)}_{s_b n_b s_a n_a; j m_j}(\theta_b \phi_b) X^{(2)BCA}_{Jb;a} \ , \tag{3.15b}$$

where

$$g^{(a,b)}_{s_b n_b s_a n_a; j m_j}(\theta_b \phi_b) = [4\pi v_b/(k_a{}^2 v_a)]^{1/2} \times \sum_{q_a q_a m_b} \hat{l}_a (l_a 0 s_a n_a \mid j_a q_a)(l_b m_b s_b n_b \mid j_b q_b) \times (j_a q_a j_b q_b \mid j - m_j) \exp[i(\sigma_{l_a} + \sigma_{l_b})] \, Y_{l_b m_b}(\theta_b \phi_b) \ . \tag{3.16}$$

The elementary cross sections used in Eqs. (2.3) and (2.16) can now be given very explicitly as

$$d\sigma^{(1)}_B(E_b;\theta_b)/d\Omega_b = [v_b/\hat{s}_a{}^2] \sum_{n_a n_b m_j} | T^{(1);B}_{s_b n_b j m_j; s_a n_a}(\theta_b,\phi_b) |^2 \ , \tag{3.17a}$$

$$d\sigma^{(2)}_{BC}(E_b,E_c;\theta_b)/d\Omega_b = [v_b/\hat{s}_a{}^2] \sum_{n_a n_b m_j} | T^{(2);BC}_{s_b n_b j m_j; s_a n_a}(\theta_b,\phi_b) |^2 \ . \tag{3.17b}$$

In order to calculate the analyzing power $A_y(\theta)$, we must be able to calculate first the cross sections for the case in which the incident beam, propagating into the z direction, is 100% polarized in the x direction, which is taken perpendicular to the scattering plane (which is taken as the y-z plane). It is given for $s_a = \frac{1}{2}$ by

$$d\sigma^{(i)}(\theta,\phi)/d\Omega = [v_b/2] \sum_{m_j n_b} | \sum_{n_a} T^{(i)}_{s_b n_b j m; s_a n_a} |^2 \ . \tag{3.18}$$

The right and left cross sections, $\sigma^{(i)}_R$ and $\sigma^{(i)}_L$, are obtained from (3.16) by setting $\delta = \pi/2$ and $-\pi/2$, respectively. The $A_y(\theta)$ is then given by

$$A_y(\theta) = \left[\sum_i (\sigma^{(i)}_L - \sigma^{(i)}_R) \right] \Big/ \left[\sum_i (\sigma^{(i)}_L + \sigma^{(i)}_R) \right] \ . \tag{3.19}$$

D. Remarks concerning practical applications

The most time consuming parts of the calculations are (i) the integration of the differential equations that appeared in (3.9), and (ii) the evaluation of the Racah coefficient $W(j_a j_b j_1 j_2; j j_c)$ of (3.11b) and the Clebsch-Gordan coefficient $(j_a q_a j_b q_b \mid j - m_j)$ of (3.16). As regards (i), we introduce in Sec. IV an approximation to speed up the calculations. As regards (ii), it should be noted that these geometrical coefficients involve angular momentum which can all become rather large (exceeding 10) simultaneously, thus preventing us from using simplifying formulas, like their asymptotic expressions. We nevertheless were able to reduce the computational time significantly, e.g., by having a large number of these coefficients calculated simultaneously, or by using some other computational techniques.

The formulas given in the preceding subsections are rather general, so that they can be used for the MSDR reactions, with a variety of combinations of particles that appear in the various channels. In practice, however, we can often use much simpler formulas. Consider, e.g., an (α,α') reaction. We then have $s_a = s_b = s_c = s_1 = s_2 = 0$, and one sees easily that many of the above formulas (and the corre-

sponding calculations) are drastically simplified. When considering the (p,p') reaction, we may choose to neglect the spin-orbit interaction in the optical potential and also to neglect the $s_1=1$ and $s_2=1$ transitions. If so, we can still use the formulas with $s_a=s_b=s_c=s_1=s_2=0$.

If we want to calculate not only the cross sections, but also the analyzing powers in the (p,p') reaction, however, we cannot neglect the spin-orbit interaction. This forces us to put $s_a=s_b=s_c=\frac{1}{2}$. We may, nevertheless, still set $s_1=s_2=0$. We may think of similar simplifications in treating other types of reactions. Continuum cross sections are rather insensitive to the use of such simplifications.

IV. MSDR CONTINUUM CROSS SECTIONS

A. Average form factors

What we have done in Sec. II is summarized by two equations, (2.3) and (2.16), which we reproduce here as

$$d^2\sigma^{(1)}(E_b)/dE_b d\Omega_b=\sum_B c_B(E_x)d\sigma_B^{(1)}(E_b)/d\Omega_b\ , \tag{4.1}$$

$$d^2\sigma^{(2)}(E_b)/dE_b d\Omega_b=\sum_{BC}\int_{E_b-Q_g^{BC}}^{E_c+Q_g^C} c_B(E_x')c_C(E_x)\{d\sigma_{BC}^{(2)}(E_b,E_c)/d\Omega_b\}dE_c\ . \tag{4.2}$$

The notation used in (4.1) and (4.2) is somewhat more general than that used in (2.3) and (2.16), in that we now have dropped the restriction to the (p,p') process. It is understood, as in Sec. III, that the channel energies in the incident and exit channels are given by E_a and E_b, respectively, and that in the intermediate channel by E_c. In (4.1) the excitation energy of the residual nucleus is related to the channel energies by $E_x=(E_a+Q_g^B)-E_b$, where Q_g^B is the Q value for the transition from the target A to the ground state of B. Similarly in (4.2), we have

$$E_x=(E_a+Q_g^C)-E_c$$

and

$$E_x'=(E_c+Q_g^{BC})-E_b,$$

where Q_g^{BC} is the Q value of the transition between the ground states of the target nuclei B and C; i.e., $Q_g^{BC}=Q_g^B-Q_g^C$. The condition that neither E_x nor E_x' should be negative dictates that the range of the E_c integration in (4.2) should be from $E_b-Q_g^{BC}$ to $E_a+Q_g^C$. It is clear that, for a pure inelastic scattering process like (p,p'), we have $Q_g^c=Q_g^{BC}=0$, reducing (4.2), e.g., to (2.16).

The MSDR continuum cross sections, expressed by (4.1) and (4.2), do look rather simple. However, actual numerical calculations to evaluate them, using directly the results of Sec. III, are still very much involved. In order to see this, we shall take the (p,p') reaction again as an example.

We shall first estimate the number N_{ph} of possible 1p-1h states $|B\rangle$. A state $|B\rangle$ is characterized by a pair of particle and hole orbits, j_p and j_h, and the total spin l; $\vec{l}=\vec{j}_p+\vec{j}_h$. The number N_{ph} is the total number of possible sets of these three quantum numbers. We may estimate that $N_{ph}\simeq 200$, if we choose the mass number of the target $A\simeq 100$, and consider only those $|B\rangle$ for which $E_B<30$ MeV or so. If we take (4.1), this means that we have to calculate about 200 $d\sigma_B^{(1)}(E_p')/d\Omega_p$, and, in order to obtain spectra, it would have to be repeated for several E_p' values. Thus, altogether it requires about 1000 calculations of $d\sigma_B^{(1)}(E_p')/d\Omega_p$. This is not unfeasible, but not trivial either. If we proceed to (4.2), the situation becomes almost intolerable. It is required that we calculate 10^5 or so of the two-step cross sections $d\sigma_{BC}^{(2)}(E_p',E_p'')/d\Omega_p$. This is considered impracticable, if not absolutely impossible.

Faced with this situation, what one might attempt to do would be to remove, in a justifiable manner, the state dependence, i.e., dependence on B and C, of the elementary cross sections $d\sigma_B^{(1)}/d\Omega$ and $d\sigma_{BC}^{(2)}/d\Omega$. From the formulas given in Sec. III, it is easy to see that such a state dependence arises because the spectroscopic amplitudes, d_J^{BC} and d_J^{BA}, and the form factors, f_J^{BC} and f_J^{BA}, are state dependent.

To remove the difficulty originating from the spectroscopic amplitudes is easy; in fact the presence of such a difficulty is only apparent. In order to see this, let us first look at Eq. (3.15a). Seen there is a summation over J, and the $X^{(1)}$ factor in the summand contains the d_J^{BA} factor, as seen in (3.11a). Among the three quantum numbers l, s, and j, specifying J, however, s is fixed (to 0 or $\frac{1}{2}$; see below), once the type of the transition is fixed. We have already stressed that $j=I_B$, which means that j is also fixed, once the final (elementary) state $|B\rangle$ is chosen. From the (known) parity of $|B\rangle$, the value of $l=j\pm s$ is also fixed. It is thus clear that the presence of the summation over J in (3.15a) is only apparent. We see that the elementary cross

section $d\sigma^{(1)}(E_b,\theta_b)/d\Omega_b$ of (3.17a) is simply proportional to $(d_J^{BA})^2$.

The matter looks somewhat more complicated for the two-step transitions. For example, (3.15b) contains a sum over C in addition to that over J. This summation over C (in the amplitude) is again only apparent, however, because, as seen in (2.16), the summation over C is to be taken only for the cross sections, and not for the amplitude. We further note that the summations over J_1 and J_2, appearing in (3.11b), are also apparent, because, in order to fully specify the final state $|B\rangle$, we have to specify what sort of elementary excitations took place in both the first and second steps. Repeating the argument we made for the one-step transitions in the preceding paragraph, we can thus conclude that a choice of a particular final state $|B\rangle$ fixes the values of J_1 and J_2 uniquely, and thus that the summations over these variables in (3.11b) are in fact absent. In other words, we can say that the elementary cross section $d\sigma^{(2)}(E_b,E_c;\theta_b)/d\Omega_b$ of (3.17b) is simply proportional to $(d_{J_2}^{BC}d_{J_1}^{CA})^2$; see (3.11b) and (3.15b).

It would be clear that these extremely simplifying features emerge because we can use, as we have justified above, the simple shell model for our calculations of the continuum spectra. There are a few limited regions in the spectra, however, in which a little more sophisticated calculations are desirable. Examples are the excitation of pairing vibrational states in two neutron (or two proton) pickup reactions, and of giant resonance states in inelastic scattering processes. There we need to use wave functions that take into account correlations. Nevertheless, how to construct such wave functions, and thus how to calculate cross sections, is well known from our experience of applying the MSDR methods to discrete state transitions. Therefore the presence of the specific type of excitations of the above examples does not cause any trouble for us in fitting the data, including the exceptional regions of narrow energy range.

To remove the state dependence of the cross sections originating from the state dependence of the form factors is a somewhat more subtle undertaking. It requires one to introduce an (additional) approximation, beyond what has been done so far. As will be explained in more detail below, the choice we decided to make is to replace f_J^{BA} by an average $\bar{f}_J$, the average being taken over the states $|B\rangle$ (or over the pair of states $|B\rangle$ and $|C\rangle$, when considering f_J^{BC}). In practice, we often make a still more drastic approximation to take an average of $\bar{f}_J$ over J, obtaining $\bar{f}$, which does not depend even on the transferred angular momentum. Since we very often use l, rather than J, to denote the total angular momentum transferred, we call $\bar{f}$ and l independent form factor (LIFF). We shall show below how drastically the calculations are simplified by using the LIFF.

If the LIFF is used, we see, e.g., in (3.9a) that the J_1 dependence on both sides disappears, and consequently, the J_1 dependence on both sides of (3.10a), and hence the J dependence of the $C_{Jb,a}^{(1)BA}$ factor in (3.11a) should be suppressed. In (3.11a), however, we never suppress the J dependence of the geometrical factor $B_J(b,a)$; we want to carry out the DWBA calculations exactly, except for the use of the LIFF. We may apply the same arguments to the two step transitions, thus suppressing the J_1 and J_2 dependences of the $C_{J_2b,J_1c,a}^{(2)BCA}$ factor, but retain these dependences in all the geometrical factors.

The fact that $d\sigma_B^{(1)}(E_b;\theta_b)/d\Omega_b$ and $d\sigma_{BC}^{(2)}(E_b,E_c;\theta_b)/d\Omega_b$ are proportional, respectively, to $(d_J^{BA})^2$ and $(d_{J_2}^{BC}d_{J_1}^{CA})^2$, which we found above, suggests that we rewrite these elementary cross sections as

$$d\sigma_B^{(1)}(E_b;\theta_b)/d\Omega_b=(d_J^{BA})^2 d\sigma_J^{(1)}(E_b;\theta_b)/d\Omega_b \ , \tag{4.3a}$$

$$d\sigma_{BC}^{(2)}(E_b,E_c;\theta_b)/d\Omega_b=(d_{J_2}^{BC})^2(d_{J_1}^{CA})^2 d\sigma_{J_1J_2;J}^{(2)}(E_b,E_c;\theta_b)/d\Omega_b \ . \tag{4.3b}$$

In writing the rhs of (4.3), we had in mind the use of the LIFF. Thus, although the new elementary cross section $d\sigma_J^{(1)}/d\Omega$ (or $d\sigma_{J_1J_2;J}^{(2)}/d\Omega$) is still dependent on the quantum number J (or J_1, J_2, and J), it is state independent. The state dependence on the rhs of (4.3) occurs thus now only through (the square of) the spectroscopic amplitude(s).

Let us introduce (4.3a) into (4.1). We then immediately see that the latter is replaced by

$$d^2\sigma^{(1)}(E_b;\theta_b)/dE_b d\Omega_b=\sum_J \rho_J(E_x)[d\sigma_J^{(1)}(E_b;\theta_b)/d\Omega_b] \ , \tag{4.4a}$$

where $\rho_J(E_x)$ is defined by

$$\rho_J(E_x)=\sum_B c_B(E_x)(d_J^{BA})^2 , \tag{4.4b}$$

and may very appropriately be called a *spectroscopic density.*

Let us next insert (4.3b) into (4.2). It is then easy to find that

$$d^2\sigma^{(2)}(E_b;\theta_b)/dE_b d\Omega_b=\sum_{J_1J_2}\int dE_c\rho_{J_1}(E_x)\rho_{J_2}(E_x')[d\sigma^{(2)}_{J_1J_2}(E_b,E_c;\theta_b)/d\Omega_b] , \tag{4.5a}$$

where

$$d\sigma^{(2)}_{J_1J_2}(E_b,E_c;\theta_b)/d\Omega_b=\sum_J d\sigma^{(2)}_{J_1J_2;J}(E_b,E_c;\theta_b)/d\Omega_b . \tag{4.5b}$$

B. Inelastic scattering

Let us first consider a simple shell-model description of elementary excitations. Then, the states excited by the one-step inelastic processes are one *ph* states specified by the angular momenta of the particle and hole orbits, j_p and j_h, and the total angular momentum $\vec{l}=\vec{j}_p+\vec{j}_h$ (and its projection m). The state $|B\rangle$ can then be written as $|B\rangle=|(j_pj_h^{-1})lm\rangle$.

We may assume an interaction of the Wigner form, given by

$$V=V(|\vec{r}_i-\vec{r}|)=\sum_{LM} v_L(r_i,r)Y^*_{LM}(\hat{r}_i) \times Y_{LM}(\hat{r}) . \tag{4.6}$$

Here, $\hat{r}$ is the coordinate of the projectile, while $\vec{r}_i$ is that of a target nucleon. Since we assumed a Wigner type interaction, there is no spin transfer, and thus we can set s_1 and s_2, and consequently s, all equal to zero. We then have $j=l$, and thus $J=(l0l)$. We shall thus write l in place of J.

By inserting (4.6) into (3.3b), and using (3.4a) and (3.4b), we find that (writing, e.g., d_l^B for d_l^{BA})

$$d_l^B=\langle j_p||i^lY_l||j_h\rangle =(-)^{l_h-j_p+l+1/2}\hat{j}_p\hat{j}_hA_{l_pl_hl} \times W(l_pj_pl_hj_h;\tfrac{1}{2}l) , \tag{4.7a}$$

$$f_l^B(r)=\int_0^\infty u_{j_p}(r')V_l(r,r')u_{j_h}(r')dr' . \tag{4.7b}$$

The geometrical factor $A_{l_pl_hl}$ in (4.7a) was defined in (3.4d). In (4.7b), the function $u_{j_p}(r)$ is the radial part of the single-particle wave function in the orbit j_p. The average form factor $\bar{f}_l$ is then defined as an average of f_l^B taken over B, i.e., over a large number of $(j_pj_h^{-1})_{lm}$ states.

In practice, however, we find that the $\bar{f}_l(r)$, thus generated, is (almost) always peaked at the nuclear surface. Therefore, we may simply approximate it by the derivative of the optical potential, a method traditionally used[16] in describing the inelastic excitation of low lying collective states. In other words, we may set

$$\bar{f}_l(r)=\beta_l\bar{f}(r) , \tag{4.7c}$$

with

$$\bar{f}(r)=R_0dU/dr , \tag{4.7d}$$

where the constant β_l may be fixed, so that the $\bar{f}_l(r)$, calculated as an average over $|B\rangle$ of (4.7b), approximately reproduces (4.7c). Note that $\bar{f}_l(r)$ still depends on l, but the dependence is only through a constant factor β_l, which may in practice be absorbed into the spectroscopic factor. We may then regard $\bar{f}(r)$ as our form factor, which is an LIFF. Using the d_l^B and $c_b(E_x)$ given, respectively, by Eqs. (4.7a) and (2.4d), and also including the β_l factor in (4.7c), $\rho_l(E_x)$ can now be given explicitly as

$$\rho_l(E_x)=\beta_l{}^2\mathrm{Im}X_l^{\mathrm{SP}}(E_x) , \tag{4.8a}$$

where $X_l^{sp}(E_x)$ is the single particle response function given as[17,18]

$$X_l^{\mathrm{SP}}(E_x)=(1/\pi)\sum_B |\langle j_p||i^lY_l||j_h\rangle|^2/[E_x-E_B-i\Gamma] . \tag{4.8b}$$

The above formalism takes the single-particle shell model literally, and one might sometimes want to use somewhat more sophisticated models. A possible candidate to use under such a circumstance is the random-phase approximation (RPA).

As is well known, the RPA describes conveniently and rather accurately the low-lying collective states, including the giant resonance states.[17–20]

The RPA equation gives rise to collective states as its solutions, and all these states put together may be used as a new set of the elementary states, which we may keep writing as $|B\rangle$'s. Application of RPA to (p,p') continuum cross sections was in fact done by Bertsch and Tsai (BT),[18] although their calculations were limited to one-step cross sections.

Even when RPA is used, most of the formulas given above can still be used just as they stand. The only modification that has to be done is to redefine $\rho_l(E_x)$, which can now be given, in terms of the RPA response function[17–19] $X_l(E_x)$, as

$$\rho_l(E_x)=\left\{\sum_B c_{B,l}(E_x)[d_l^{\alpha}]^2\right\}$$

$$=C_l{}^{-1}\mathrm{Im}X_l(E_x)\ , \tag{4.9a}$$

with

$$C_l=\pi R_0{}^2\int(d\rho_{\mathrm{matter}}/dr)r^{l+2}dr\ , \tag{4.9b}$$

$$X_l(E_x)=(1/\pi)\sum_B[E_x-E_B-i\Gamma]^{-1}\,|\,Q_{Bl}\,|^2\ , \tag{4.9c}$$

$$|\,Q_{Bl}\,|^2=|\,\langle\phi_l^B||r^lY_{lm}||0\rangle\,|^2\ . \tag{4.9d}$$

In (4.9c), E_B now stands for an RPA eigenenergy, corresponding to the eigenstate $|\phi_l^B\rangle$, in terms of which the matrix elements Q_{Bl} are given. C_l in (4.9a) are given by (4.9b), and take into account the defuseness of the nuclear matter distribution, $\rho_{\mathrm{matter}}(r)$.

We have used both *ph*-pair[6] and RPA (Ref. 9) descriptions and noticed that the results were better when the latter was used; see Sec. V. In our more recent calculations, however, we started to notice that the use of the LIFF leads to somewhat unsatisfactory results, in particular when analyzing power was also calculated. We thus have decided to carry out a fully microscopic calculation (at least for the one-step contributions), and we expect to obtain the final results shortly. In any case, the explanation of these new calculations is somewhat lengthy, and we plan to discuss them in a separate paper,[21] although we present in Sec. V some of our preliminary results.

C. Reactions involving nucleon transfer

Let us take the (p,α) reaction as an example of the reactions that involve nucleon transfer steps. This reaction has the unique value of $s=\frac{1}{2}$, and thus $j=l\pm\frac{1}{2}$. We shall thus use the index (lj) in place of J.

As is well known from the DWBA theory applied to discrete state transitions, the form factor $f_{lj}^B(r)$ may be taken as the radial wave function, describing the motion, in the target, of the center of mass of the three nucleons, $(2n+p)$, to be picked up in the reaction. On the other hand, the spectroscopic amplitude d_{lj}^B may be understood as the amplitude with which the wave function of the above three nucleons contains a component that is described as the triton *internal* wave function times $f_{lj}^B(r)$. [Note that our $f_{lj}^B(r)$ is understood to include the so-called N_0 factor, well known in the zero-range DWBA theory.[1]]

The degree of sophistication used in obtaining d_{lj}^B and $f_{lj}^B(r)$ varies widely even when DWBA is applied to discrete-state transitions. However, it is not too unusual to obtain $f_{lj}^B(r)$ as the wave function of a triton, treated as an elementary particle bound in a Woods-Saxon type potential, with an appropriately chosen binding (separation) energy. If we choose an E_x, we know the separation energy to be used. Corresponding to this E_x, we may also find a median value for (lj), and obtain the triton wave function for this median (lj). If we use this wave function, $\bar{f}(r)$, irrespective of the actual (lj) (and of course of B), it can be considered the LIFF for the (p,α) calculations. This we do in practice.

We shall now explain how to obtain d_{lj}^B for our purpose. Once we decide to use LIFF, it does not make much sense to try to obtain d_{lj}^B based on very sophisticated models. Just as we considered a pure *ph* model in Sec. IV B, we shall use the simple shell model again here. In fact, we may go one step further to assume that the harmonic-oscillator shell model (HOSM) can be used.

Let us assume that, in the target, the least bound neutron(s) and proton(s) are in orbits whose total oscillator quantum numbers are, respectively, N_n and N_p. Suppose that we pick up three nucleons from orbits whose quantum numbers are N_1, N_2, and N_3, with $N_1+N_2+N_3=\Lambda$. Then the excitation energy E_B of the thus formed $3h$ state is nothing but $\hbar\omega\bar{N}$, where $\bar{N}=(2N_n+N_p)-\Lambda$. In other words, in order to form a state at $E_B=\hbar\omega\bar{N}$, we should pick up three nucleons from orbits so as to make $\Lambda=(2N_n+N_p)-\bar{N}$. For a large Λ, there can be many combinations of the triads (N_1,N_2,N_3). Further, for a given N_i, there are several combinations of the principal and orbital quantum numbers that satisfy $N_i=2n_i+l_i$. Therefore, for a given Λ, there can be a rather large number of elementary states,

and they are all degenerate at $E_B=\hbar\omega\bar{N}$.

Because of this degeneracy, the $c_b(E_x)$ factor in the summand of (4.4b) is independent of B, when summed over those with a fixed Λ. We may thus rewrite $c_B(E_x)$ as $c_\Lambda(E_x)$, with the understanding that $c_\Lambda(E_x)$ is given, e.g., by (2.4c) by using $\hbar\omega\bar{N}$ for E_B in it. Equation (4.4b) may now be replaced by

$$\rho_{lj}(E_x)=\sum_\Lambda c_\Lambda(E_x)\sum_{B\in\Lambda}[d_{lj}^B]^2 . \tag{4.10a}$$

The restriction $B\in\Lambda$ in the summation over B in (4.10a) will be clear from what we explained above. The summation over Λ is understood to obey also a restriction that $\Lambda\geq l$ and $(-)^\Lambda=(-)^l$.

As pointed out in Ref. 7, we can use the technique developed by Ichimura *et al.*,[22] in carrying out analytically the B sum in (4.10a). We find that (4.10a) can be replaced by

$$\rho_{lj}(E_x)=\sum_\Lambda c_\Lambda(E_x)\times\sum_{N_1+N_2+N_3=\Lambda}[G_\Lambda(\{N_i\})]^2 , \tag{4.10b}$$

with

$$G(\{N_i\})=3^{-\Lambda/2}N(\{N_i\})\times[\Lambda!/(N_1!N_2!N_3!)]^{1/2} , \tag{4.10c}$$

where $N(\{N_i\})=\sqrt{6}$, $\sqrt{3}$, or 1, depending on whether all the N_i's are different, two of them are equal, or all of them are equal.

The second sum in (4.10b), of course, means a threefold summation over N_1, N_2, and N_3, but with a restriction that $N_1+N_2+N_3=\Lambda$. It is interesting to note that the result of this summation simply equals unity, if all the orbits $\{N_i\}$ that satisfy $N_1+N_2+N_3=\Lambda$ are occupied, and thus can contribute to the (p,α) reaction. (This is nothing but a statement of completeness of the oscillator states.) It will be clear that this happens for relatively small Λ, the picking up of the nucleons taking place mostly from low lying orbits.

It will be obvious that, with the HOSM we are using, the upper limit of Λ, and hence that of l, equals $2N_n+N_p$. When Λ equals, or is very close to, this upper limit, corresponding to very low E_x, only a few of the set $\{N_i\}$ will satisfy $N_1+N_2+N_3=\Lambda$, thus making the second sum of (4.10b) much smaller than unity. This simply reflects the fact that, for a lower excitation, the level density is relatively low. A feature which is unusual, nevertheless, is the fact that, for a fixed l, the level density decreases as E_x increases. This unusual feature appears because we are counting the level density of the $3h$ states, not that of the whole nuclear system, as used, e.g., in the evaporation calculations.

D. Remarks on numerical calculations

Our numerical calculations are performed based on Eqs. (4.4a) and (4.5a). Thanks to the use of the LIFF, they are now in a form much simpler than they otherwise could be. Yet the numerical calculations to be performed are not trivial. We shall give some idea of the numerical task which is involved.

Let us take for simplicity the case with $V_{so}=0$. We can then set $s_a=s=s_c=0$, as noted above, which makes various expressions very simple. We, in particular, find that the pair of inhomogeneous equations in (3.9) take the following very simple form, in spite of the fact that we now write all the quantum numbers explicitly:

$$D_{l_b}\chi_{l_bl_a;l_1}(r)=\bar{f}(r)\chi_{l_a}(r) , \tag{4.11a}$$

$$D_{l_b}\chi_{l_bl_cl_a;l_2l_1}(r)=\bar{f}(r)\chi_{l_cl_a;l_1}(r) . \tag{4.11b}$$

They are to be solved with the boundary condition (for $r\to\infty$) given, respectively, by

$$C^{(1)}_{l_bl_a;l_1}[\exp(-i\sigma_{l_b})H^{(+)}_{l_b}]$$

and

$$C^{(2)}_{l_bl_cl_a;l_2l_1}[\exp(-i\sigma_{l_b})H^{(+)}_{l_b}] ;$$

cf. (3.10). Contrary to the practice of Sec. III, we have written the orbital angular momenta l_a, l_b, and l_c explicitly in (4.11).

For a given l_a, (4.11a) is to be solved for all l_b that satisfy the selection rules given by $\vec{l}_a+\vec{l}_b+\vec{l}_1=0$ and $l_a+l_b+l_1=$even. Unless l_a is very small, this means that (4.11a) has to be solved l_1+1 times (for each l_a). This is to be repeated for all l_1 ranging from 0 to $l_1^{\max}$, if $f(r)$ depends on l_1. Therefore, we have to solve (4.11a)

$$(l_1^{\max}+1)(l_1^{\max}+2)/2$$

times altogether. The use of LIFF, as done actually in (4.11a), however, reduces this number to $l_1^{\max}+1$, which is significant, since $l_1^{\max}$ often exceeds 10. [With LIFF, the l_1 dependence of $\chi_{l_bl_a;l_1}$ could have been suppressed. We retained it, in order to clarify the above selection rules. The same is true for $C^{(1)}$,

and for the $(l_2 l_1)$ dependences of $\chi_{l_b l_c l_a; l_2 l_1}$ and of $C^{(2)}$.]

In a similar way we find that we have to solve (4.11b) $l_2^{\max}+1$ times, for a given pair of l_a and l_c, where $l_2^{\max}$ is the maximum value of l_2. Thus with LIFF, we have to solve an inhomogeneous equation [of the form of (4.11)]

$$l_a^{\max}\times(l_1^{\max}+1)\times(l_2^{\max}+1)$$

times, in order to obtain the whole set of $C^{(2)}_{l_b l_c l_a}$ which we need to evaluate all the two-step cross sections, where $l_a^{\max}$ is the maximum value of l_a. With the CDC-CYBER-170/750 computer at the University of Texas, we found that these calculations took about 1 min.

The two-step cross sections are calculated by using these $C^{(2)}$'s in (3.11b), and then using (3.15b) and (3.17b), and we found that this part of the calculations took another 1 min, a major fraction of the time being spent in evaluating the Racah coefficient $W(l_a l_1 l_b l_2; l_c l)$ that appears in (3.11b). Note that, since all the six angular momenta that appear as the argument of this Racah coefficient take, on the average, ten different values independently, about one million Racah coefficients have to be evaluated. The appearance of large l_1, l_2, and l is characteristic of the present MSDR calculation of the continuum cross sections. This will seldom (or never) be experienced in MSDR calculations for discrete state transitions.

Thus, it takes about 2 min to complete the two-step calculations. This is, however, for a given pair of energies (E_b,E_c). As will be explained shortly, our computer program ORION-1 is designed to calculate two-step cross sections for six pairs of (E_b,E_c). Therefore, we need 10–15 min altogether to calculate all the two-step cross sections. Compared with this, the time needed for one-step cross sections is almost negligible, being of the order of 10 s.

The above estimate of the computational time was made for the case with $V_{so}=0$. If $V_{so}\neq 0$, the l_a that appears in (4.11a) has to be replaced by $(l_a j_a)$, and similarly for l_c and l_b. This means that the number of times with which we have to solve the inhomogeneous equation of (4.11) is increased by about a factor of 8, compared with what we gave above, making the total time needed exceed 1 h. The ORION-1 program was thus designed so that the actual calculations are done only for even values of l_1 and l_2 [which restricts (4.11) to cases with $(-)^{l_a}=(-)^{l_b}=(-)^{l_c}$], the cross sections involving odd value(s) of l_1 and l_2 being obtained by interpolation. The total time needed was thus cut back to 20 min or so.

Suppose we want to obtain $\sigma^{(1)}(E_b)$ for E_b ranging from $E_b^{\min}$ to $E_b^{\max}$. Since the E_b dependence of $\sigma_l^{(1);\mathrm{DW}}(E_b)$ was rather weak, we found it sufficient to evaluate it accurately (for each l) at three values of E_b: $E_b^{\max}(=E_{b1})$, $(E_b^{\max}+E_b^{\min})/2(=E_{b2})$, and $E_b^{\min}(=E_{b3})$, and obtain their values at other E_b by a logarithmic interpolation. The thus obtained $\sigma_l^{(1)}(E_b)$ are then combined with $\rho_l(E_x)$ in (4.4a) to obtain $\sigma^{(1)}(E_b)$ at any desired E_b. The evaluation of $\rho_l(E_x)$ is done by using (4.4b). This part of the calculation is rather easy to make, because, although (4.4b) contains a lengthy sum over B, the summands are evaluated very easily.

As for the two-step cross sections, we evaluate $\sigma^{(2)}_{l_2 l_1 l}(E_b,E_c)$ accurately (for all l_2, l_1, and l) for six pairs of (E_b,E_c): (E_{b1},E_{c1}), (E_{b2},E_{c1}), (E_{b3},E_{c1}), (E_{b2},E_{c2}), (E_{b3},E_{c2}), and (E_{b3},E_{c3}), where $E_{c1}=E_a+Q_g^{\alpha}$, $E_{c3}=E_b^{\min}-Q_g^{\beta}$, and $E_{c2}=(E_{c1}+E_{c3})/2$. These points define a triangle in the (E_b,E_c) plane, and the $\sigma^{(2)}_{l_2 l_1 l}(E_b,E_c)$ point inside this triangle can be obtained by a two-dimensional logarithmic interpolation.

Actually, this interpolation needs to be done only for $\sigma^{(2)}_{l_2 l_1}(E_b,E_c)$ after carrying out the l sum of (4.5b) at the above six points. Once done, we can carry out the E_c integral of (4.5a) [assuming that $\rho_{l_1}(E_x)$ and $\rho_{l_2}(E_x')$ have been prepared in advance], to obtain $\sigma^{(2)}(E_b)$ for any E_b ranging from $E_b^{\min}$ to $E_b^{\max}$.

V. NUMERICAL RESULTS AND COMPARISON WITH EXPERIMENT

A. (p,p') reactions

The first application of our MSDR method developed in Secs. II–IV was made for ^{27}Al(p,p') and ^{209}Bi(p,p') data by Bertrand and Peelle,[23] taken with $E_p=62$ MeV, and the results[6] are reproduced here as Fig. 1.

In this figure, the sum of one- and two-step cross sections is represented by solid lines, and as seen, it reproduces very nicely both the angular and energy distributions found in experiment. The fit obtained simultaneously for ^{27}Al and ^{209}Bi shows that the mass dependence is also correctly predicted.

We show in Fig. 1, with dotted lines, also the theoretical cross sections obtained when only the one-step cross sections $\sigma^{(1)}$ were considered. As expected, the difference between the solid and the dot-

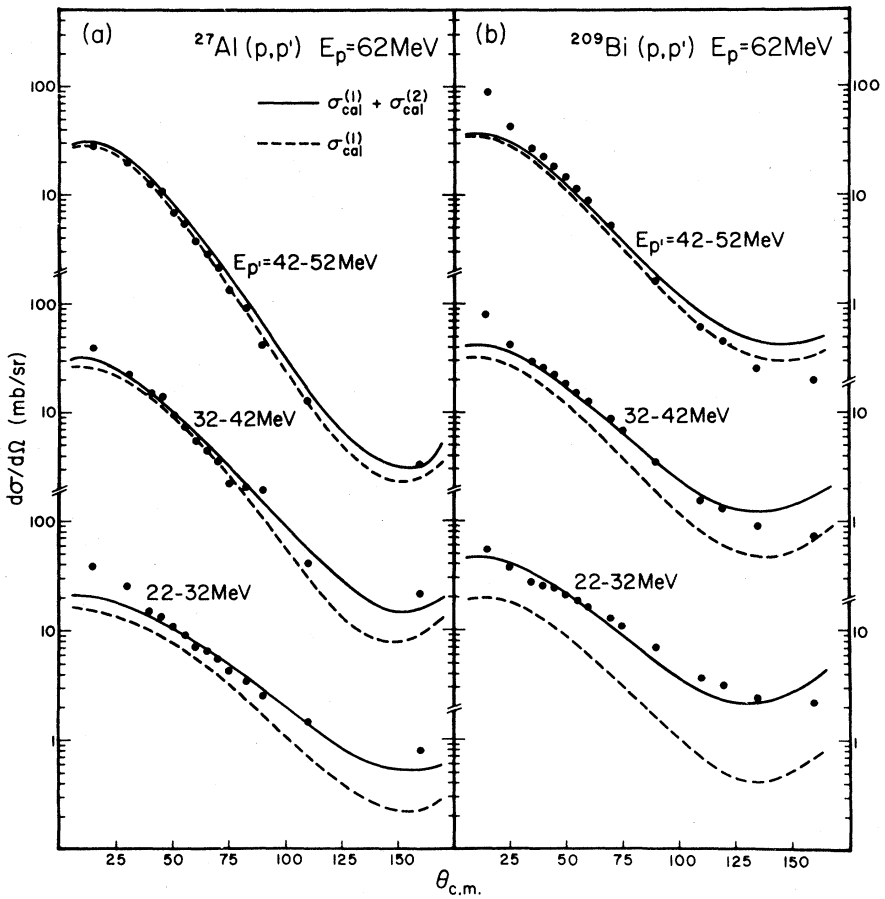

FIG. 1. Comparison of the calculated (p,p') cross sections summed over the 10 MeV energy bin shown with the corresponding experimental data. The data were taken from Ref. 23. The solid lines represent the sum of one- and two-step cross sections, while the dotted lines represent only the one-step cross section.

ted lines, i.e., the contribution of the two-step cross sections $\sigma^{(2)}$, increases as E'_p decreases, making $\sigma^{(2)}$ the dominant component for the lowest E'_p. In fact, $\sigma^{(2)}$ accounts for about 80% of the total cross section for $E'_p = 22-32$ MeV at large angles when ^{209}Bi is taken as the target.

In spite of the good overall fit shown in Fig. 1, our theory is not completely free from trouble. Take, e.g., the ^{209}Bi case, and look at the $E'_p = 42-52$ MeV and $32-42$ MeV angular distributions. As the angle θ is decreased, the experimental cross section keeps increasing, but the theoretical cross section flattens off for $\theta < 30°$, making the discrepancy at the smallest angle, $\theta = 15°$, as large as a factor of 2 to 3. We shall discuss this *small-angle problem* later.

Another point, which is not seen offhand from Fig. 1, concerns the absolute magnitude of the cross sections. We note that the calculations of Ref. 5 used the *ph*-pair states as elementary states, and also the LIFF of (4.7c). In using (4.7c), we fixed the values of β_l in such a way that the resultant LIFF represents as close as possible the average of $f^{\beta}(r)$. The results of Fig. 1, obtained by using these β_l, agreed with the data even in magnitudes.

When the LIFF of (4.7c) is used, however, it is possible to test the validity of the β_l values thus employed. It is to see whether the energy-weighted sum rule (EWSR) (Refs. 18 and 24) is obeyed or not. As noted by Tsai and Bertsch,[25] the β_l's we used in Ref. 6 were somewhat too large, exceeding the EWSR by a factor of about 2 for $l \leq 4$. When these β_l's were reduced, to satisfy the EWSR, the theoretical cross sections were reduced accordingly.

As discussed in Sec. IV B, we might improve the situation by switching to the use of the RPA states as elementary states. We thus performed in Ref. 9 calculations with RPA, and obtained some, but not sufficient, improvement. (In Ref. 9, we stated that the use of RPA solved the above *magnitude problem*. Unfortunately, this conclusion was too premature; we later found an error in the calculations re-

ported there.)

In spite of these problems, the rather good overall fits to data achieved in Refs. 6 and 9 seem to suggest that our approach formulated in Secs. II and III is basically correct. The source of the trouble might then be traced to the use of somewhat oversimplifying approximations introduced in Sec. IV; in particular, the use of the LIFF. If it is indeed the case, a possible way out is to switch to fully microscopic calculations, which means to stay, e.g., with Eqs. (4.1) and (4.2), without a further simplification. Note that several authors[26] have investigated microscopic calculations, although their use was limited to discrete state transitions.

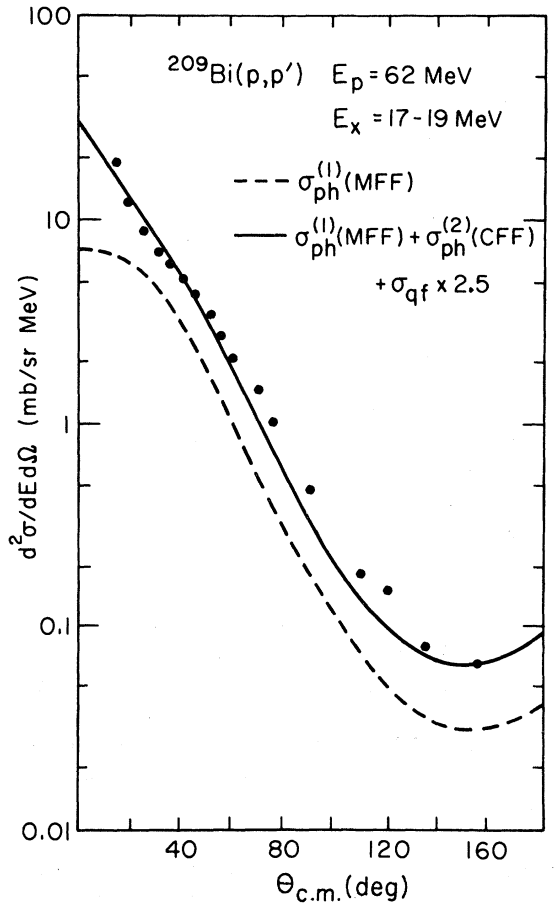

FIG. 2. Comparison of the calculated (p,p') cross sections summed over the 2 MeV energy bin shown with the corresponding experimental data. The data were taken from Ref. 23. The dotted line represents the one-step cross section obtained by using the microscopic form factor, while the solid line was obtained by adding, to this one-step cross section, the two-step cross section estimated in the way explained in the text, and also the contribution from the (p,d^*) process.

Since we are to use microscopic form factors (MFF), we shall refer to these calculations as MFF calculations, as opposed to LIFF calculations, which may also be called CFF calculations because of the use of the collective form factors, as seen in (4.7d). Our investigations of the use of the MFF are still underway,[21] but a few interesting preliminary results have nevertheless been obtained. In these preliminary calculations, we used the *ph*-pair states, rather than the RPA states. Also the MFF calculations were done only for one-step transitions.

We show in Fig. 2 a result of such calculations for the ^{209}Bi(p,p') reaction, with $E_x = 17-19$ MeV, just above the giant-resonance region. The dashed curve in Fig. 2 represents the one-step cross section, obtained as a sum of about 200 microscopic cross sections, pertaining to various *ph* pairs and to l's that range from 0 to 10. As is seen, the cross section underestimates the experiment by an angle-dependent factor, whose value ranges from 1.7 to 3. We know, however, that increased theoretical cross sections are obtained if we switch to the use of the RPA states, and then add two-step contributions. The (angle-dependent) increment factor, with which the thus obtained final cross section would exceed the above one-step cross section, can be estimated from our previous calculations.[6,9]

Multiplying the one-step cross sections in Fig. 2 with the thus estimated increment factor, and further adding the (p,d^*) cross sections, to be explained below, we obtained the cross section represented by the solid line in Fig. 2. As is seen, it agrees with the data at all angles, thus removing both the small-angle and the magnitude problems. As will be clarified shortly, the small-angle problem was removed by the addition of the (p,d^*) cross sections. On the other hand, the magnitude problem was removed by the use of the MFF.

Note that to obtain increased (one-step) cross sections by the use of MFF does not contradict the requirement imposed by the EWSR, which can be defined only when LIFF is used. We have normalized the strength of the two-body interaction, out of which the MFF was constructed, so that we could fit the experimental cross section exciting the collective 3^- state (at 2.61 MeV). With the use of this interaction, we found that the MFF one-step cross sections were 30% or so larger than the corresponding LIFF one-step cross sections (with the LIFF constructed so as to be consistent with the EWSR), considering in both cases only the excitation of normal parity states. With the MFF, we also have cross sections exciting non-normal parity states (which we did not have with the LIFF), which

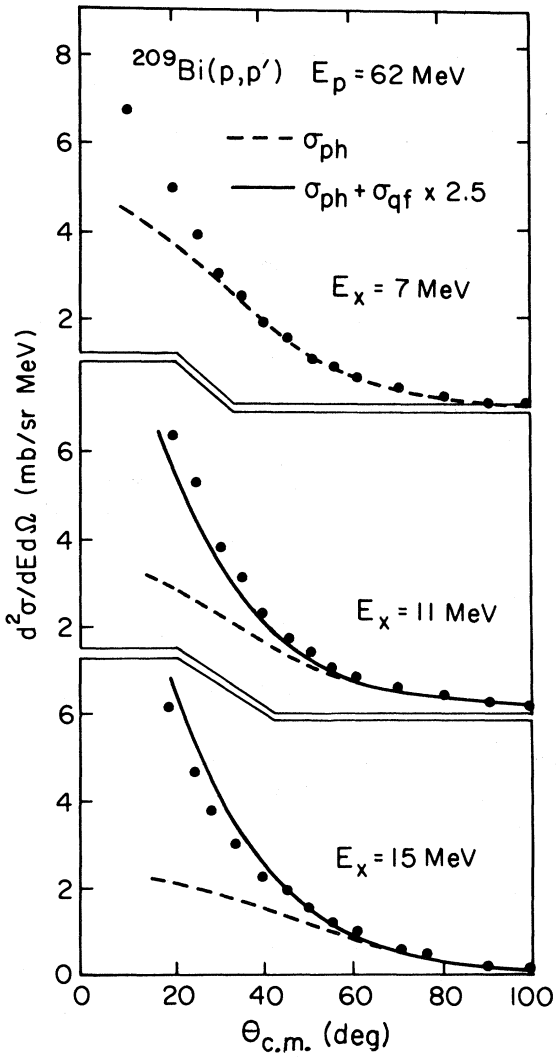

FIG. 3. Comparison of the calculated (p,p') cross sections with the experimental data of Ref. 23 at $E_x = 7$, 11, and 15 MeV. The differences between the solid and dashed lines represent the (p,d^*) cross sections.

turned out to be close to half of the cross sections for exciting the normal parity states. Combining these two sources of increments, we found that the one-step MFF continuum cross sections were nearly twice as large as were the corresponding LIFF cross sections. This is why the use of the MFF removed the magnitude problem, which was not possible with the LIFF.

We shall now explain what is meant by the (p,d^*) cross sections. They are interpreted as the proton-singles cross sections that result from one-nucleon pickup processes. Contrary to the usual (p,d) reactions, however, we consider that the resultant systems $(2p)$ or (pn), which we collectively denote by d^*, are in metastable states, and thus eventually decay into two nucleons. It is known that, for E_p as high as 62 MeV, the (p,d) cross section leading to a low-lying discrete state is rather small, because of a very severe momentum mismatch. When the internal energy of the d^* becomes appreciable, however, the c.m. energy of d^* relative to the residual nucleus is reduced accordingly, making the (p,d^*) reaction rather well matched. It is thus expected that the (p,d^*) cross section can become appreciable. How large they really are is seen in Fig. 3.

The dashed lines in Fig. 3 correspond to the cross sections that were represented by the solid line in Fig. 2, except that the (p,d^*) cross sections have not yet been added. As is seen, they fit the data nicely at larger angles, but underestimate the experiment severely at smaller angles, revealing the small-angle problem. If we add the (p,d^*) cross sections, however, we obtain the total cross sections, represented by the solid lines in Fig. 3, which now agree very well with experiment. It is thus seen that the consideration of the (p,d^*) processes indeed solves the small-angle problem. We remark here that we have discussed this on two earlier occasions.[11,13] We further note that Holmgren *et al.*[27] also discussed this, although they used plane waves, rather than distorted waves, in their discussion.

In presenting the (p,d^*) contributions in both Figs. 2 and 3, we multiplied, by a factor of $N = 2.5$, the cross sections that were obtained from the calculations explained above. This factor should not, however, be regarded as an arbitrary factor. Recently, theories[28,29] were developed on how to calculate the singles cross sections in processes in which the intermediate state is a three-body system, just as here we have the d^* plus the residual-nucleus system. Take, e.g., the case in which $d^* = p + n$. What we have calculated, in the way described above, were only the cross sections for the processes in which both p and n fly away. There occur, however, also processes in which the n is recaptured by the residual nucleus, and it can also contribute to the proton singles cross sections. We showed[29] that this direct reaction followed by fusion (DRF) cross section can be very large. Although we have not done the DRF calculation for the present (p,d^*) process, it is very likely that the above factor $N = 2.5$ is explained this way.

We have discussed so far only the (p,p') cross sections. Very recently, however, Sakai *et al.*[30] measured the analyzing power, A_y, by using a 65 MeV $\vec{p}$ beam, and we have analyzed this new data as well, although it is preliminary in the same sense as is the result presented in Fig. 2.

We compare in Fig. 4 our results with experi-

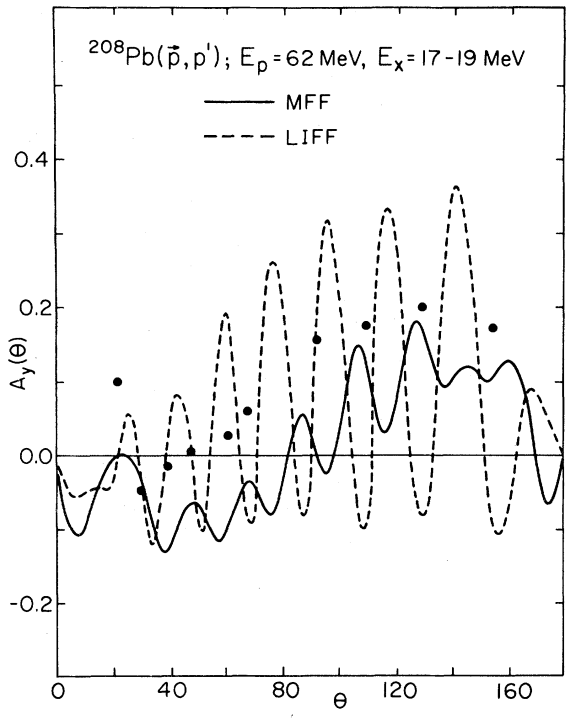

FIG. 4. Comparison of the calculated analyzing power of the (p,p') reaction with experiment of Ref. 30. The solid line represents the analyzing power calculated by using the microscopic form factor, while the dotted line is that obtained by using the collective form factor.

ment, again with a ^{208}Pb target and for $E_x = 15 \sim 17$ MeV, as in Fig. 2. As is seen, the results of the MFF calculations, presented by the solid line, agree rather nicely with experiment, showing that our method is capable of fitting data, even data as subtle as A_y. It should, nevertheless, be kept in mind that we used the *ph* states as the elementary states. The use of the RPA states, the addition of two-step contributions, and so forth, might modify the results somewhat. Note also that the calculation was done for $E_p = 62$ MeV, while the data[30] were taken with $E_p = 65$ MeV.

Figure 4 also shows, as a dotted line, the results obtained with LIFF, and of course with $V_{so} \neq 0$. It is seen that the resultant A_y oscillates very violently, with amplitudes far too large compared with experiment. When the LIFF is used, contributions from different l seem to behave too similarly.

The results of more sophisticated MFF calculations[21] may differ somewhat from the above preliminary results, but it seems unlikely that the difference is drastic. Assuming that it is indeed the case, one statement we may make, based on the above results, is that the magnitudes of the (p,p') continuum cross sections are accounted for by the calculations based on the MSDR theory. This conclusion contradicts that of Bertsch and Tsai (BF),[18] who stressed that the DR theory predicted cross sections too small to account for the experimental magnitudes. We note, however, that BF calculated the spectrum only at 20°, where, as we showed above, the cross section is dominated by that of the (p,d^*) process. BF did not consider this process. They also did not consider the two-step processes, which are not so small at higher E_x, even at angles as small as 20°. Our cross sections at 20° were nearly one order of magnitude larger than were those of BF. It is thus seen why two contradictory conclusions were drawn.

In concluding this subsection, we note that all the calculations we discussed in this subsection were performed by using the optical potential parameters proposed sometime ago by Menet *et al.*[31]

B. (p,n) reaction

As the second example of applying our method, we chose the ^{208}Pb(p,n) reaction, taken with $E_p = 45$ MeV.[32] The calculation was done some time ago,[8] by using the very simple-minded LIFF of the type given by (4.7c). We have not attempted since then to replace this earlier calculation by more sophisticated calculations, as was done for the (p,p') reactions, and was explained in Sec. V A.

Very little modification needs to be made in going from the (p,p') to the (p,n) calculations. In the calculations of Ref. 8, we considered the one-step, (p,n), and the two-step, (p,n,n') and (p,p',n) processes. The treatment of the inelastic steps, (n,n') and (p,p'), involved in these two-step processes, was done in exactly the same way as it was in Ref. 6. In particular, we used (4.7c) for the form factor, with $\beta_l = 0.028$ for $l = 0$ and 2, and $\beta_l = 0.023$ for $l = 3-6$; we found it unnecessary to consider l beyond 6.

As regards the (p,n) step of the reaction, one modification we had to make was to replace the spectroscopic density, which had been constructed corresponding to the creation of the *ph* pairs (of the same kind of nucleons), by that corresponding to the creation of the proton-particle–neutron-hole pairs. One can easily see that the formulas given by Eqs. (4.6) and (4.7) can be used again for this purpose. As for the form factor, we did not use[8] (4.7c), but $\bar{f}_l(r) = \beta_l \mathrm{Re}(U)$, i.e., the real part of the Woods-Saxon potential multiplied with $\beta_l = 0.0038$ for $l = 0-2$, and $\beta_l = 0.003$ for $l = 3-6$. Note that the ratio $(\beta_l)^{(pn)}/(\beta_l)^{(\mathrm{inelastic})}$, of the β_l's, reproduces

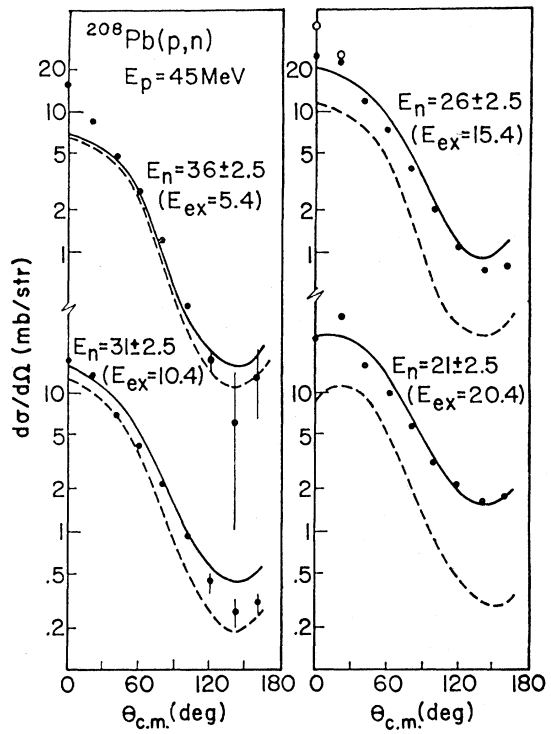

FIG. 5. Comparison of the calculated (p,n) cross sections with experiment of Ref. 32. The solid lines represent the sum of the one- and two-step cross sections, while the dotted lines represent only the one-step cross section.

(approximately) the ratio of the strengths of the $T=1$ and $T=0$ components, known for the effective two-body interactions. As for the optical model parameters, we used those of Refs. 31 and 33 for proton and neutron channels, respectively.

The results of the calculations thus performed[8] are reproduced in Fig. 5. As was the case, e.g., in Fig. 1, the solid lines represent the sum of one- and two-step cross sections, while the broken lines include only the one-step cross sections. As is seen, the solid lines fit the data very well. It is also seen that the dashed lines underpredict the data, in particular for lower E_n and larger $\theta_{\text{c.m.}}$. All these features are very much the same as they were in Fig. 1.

In fact, we observe one more very interesting similarity between Figs. 1 and 5. Regarding Fig. 1, we pointed out the presence of a trouble, which we called a small-angle problem. One then sees that the same problem also reveals itself in Fig. 5. In Sec. V A, we showed that the problem was nicely removed by considering the (p,d^*) contributions. One may very well expect that the same recipe applies here too.

We also note that the magnitude problem that we encountered with the results in Fig. 1, is encountered here again, because the β_l values we used for the inelastic steps (see above) are the same as those used in Ref. 6, and thus (apparently) contradict the EWSR. However, what we showed in Sec. V A was that the more sophisticated calculations, using the RPA and MFF, justified the calculations of Ref. 6. The same argument can be used here again to justify the calculations of Ref. 8. We may thus be able to say, to the same extent as we did in Sec. V A, that our MSDR calculations fit the continuum (p,n) data, including the magnitudes.

C. (p,α) reactions

In Fig. 6, we have reproduced our (p,α) analysis, reported earlier in Ref. 7. In the left-hand column of this figure, the angular distributions of the observed cross sections[34] (taken originally with 1 MeV intervals, which we integrated over 4-MeV widths) are compared with the calculations. The results represented by dashed lines include only the one-step (p,α) processes, and are seen to underpredict experimental values significantly, particularly for lower E_α. When two-step contributions are added, however, the theoretical cross sections are replaced by those represented by solid lines, which are in good agreement with experiment.

In the right-hand column of Fig. 6, we give spectra taken at several angles. One again sees good agreement with experiment for higher E_α, but notices a significant discrepancy at lower E_α. This discrepancy was caused, however, simply because we neglected the evaporation components. Later, we performed a Hauser-Feshbach type calculation, and found that this discrepancy was easily removed. Discrepancies are also noticed in the smaller angle spectra, at around $E_\alpha=45$ MeV; theory failed to produce a shoulder which experimental spectra had in this energy region. This, we believe, is due to an excitation of the pairing-vibrational state (caused by a picking up of a correlated neutron pair; a proton, which is also picked up, is playing the role of a spectator). We also found that the gap was easily filled by adding the contributions of this specific mode.

Recently, Dragun *et al.*[35] used the formalism we presented in Ref. 7, and analyzed ^{93}Nb(p,α) and ^{118}Sn(p,α) data.[36] Our analysis dealt with protons with $E_p=62$ MeV, while in the case of Dragun *et al.*, E_p was 44.3 and 34.6 MeV. Because of the lower E_p, it appears that they were able to obtain

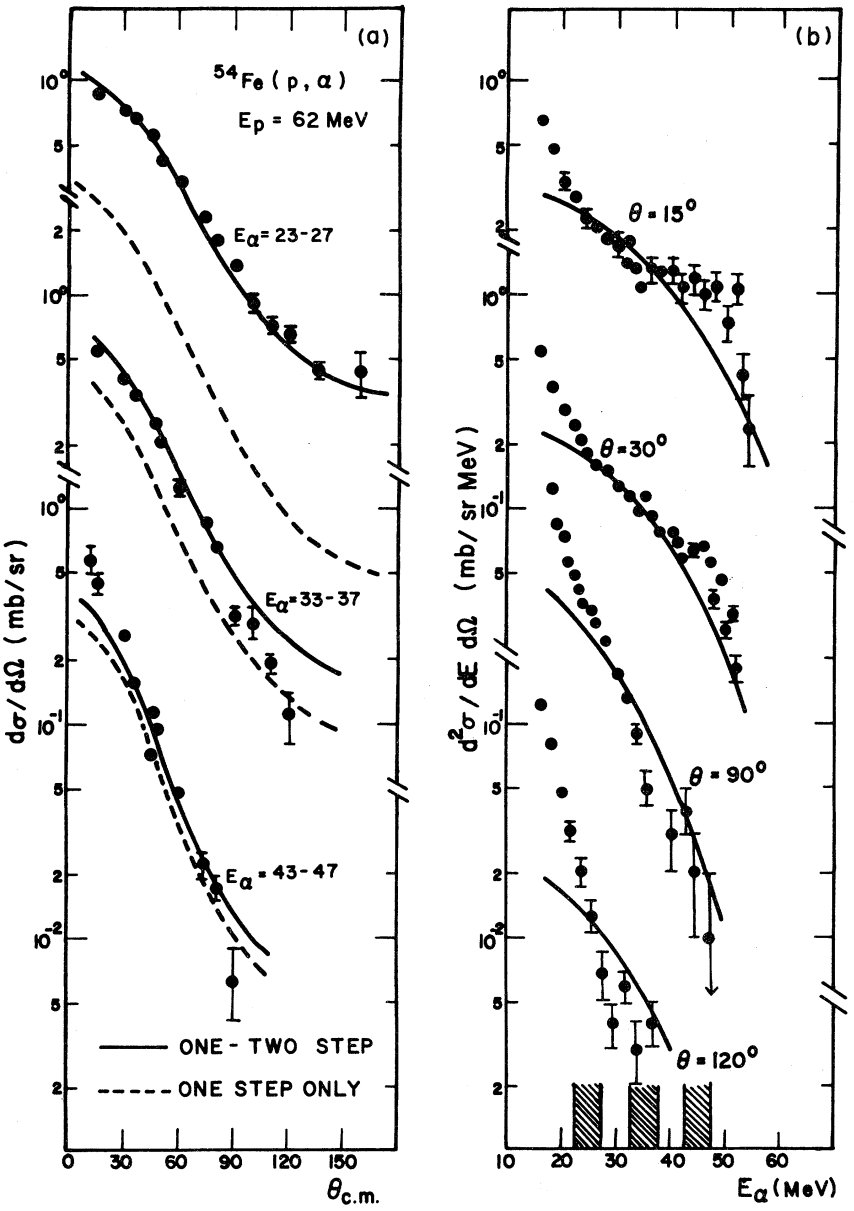

FIG. 6. Comparison of the calculated (p,α) cross sections with experiment of Ref. 34. In both (a) and (b), the solid lines represent the sum of the one- and two-step cross sections, while the dotted lines in (a) represent only the one-step cross section.

good agreement with the data by considering only the one-step direct reaction contributions, and those of the Hauser-Feshbach processes. See a few figures in Ref. 35, where one finds that the agreement with data achieved is indeed very good. One nevertheless sees that the theory underpredicted the data slightly, for smaller E_α and larger θ, indicating that the two-step processes may not be entirely negligible, even for the lower E_p.

We shall now proceed to the analysis of the A_y data[30] in the (p,α) continuum; see also Ref. 37 for similar data. Since the data were taken[30] with $E_p=65$ MeV, we will have to consider at least one- and two-step processes, as we did in Ref. 7. Regarding the two-step processes, we may take the (p,α,α') and the (p,p',α) as two of the most important two-step processes. In Ref. 7, however, we calculated accurately only the (p,α,α') cross sections, and multiplied them by a factor of 4 before adding them to the one-step (p,α) cross sections. The multiplication by factor 4 was done with the assumption that the (p,p',α) process would behave very

similarly as does the (p,α,α') process, and that these two processes would interfere constructively.

Before starting the analysis of A_y, we first tested the validity of the above assumption, and found that (p,α,α') and the (p,p',α) processes did not behave so similarly, contrary to what we had thought.[7] (See below.) We also noticed that, in the framework of our calculations, it was more reasonable to consider that these two processes do not interfere, than to consider them to interfere. To see this, it is sufficient to look back, e.g., at Eq. (2.13). As is seen, once a mode of transition is chosen, the continuum cross section is given as a sum over states $|B\rangle$ and $|C\rangle$ (in addition to having an integration over E_x corresponding to the energy of $|C\rangle$). In other words, Eq. (2.13) holds separately for the (p,α,α') and (p,p',α) processes, in the present example, and thus there is no way for them to interfere. The absence of the interference resulted because the states that are actually excited are complicated nuclear eigenstates, not the simple elementary states which allowed us to use statistical arguments to arrive at Eq. (2.13).

In carrying out the calculations, we used the (energy dependent) optical model parameters of Menet *et al.*[31] and of Sheperd *et al.*,[38] respectively, for the proton and the α channels. The calculations were performed, for simplicity in manipulating the spectroscopic densities, for the ^{90}Zr(p,α), rather than the ^{93}Nb(p,α) reaction of Ref. 30. The ground state Q value for the ^{90}Zr(p,α) reaction is $Q_{gr}=6$ MeV.

Following the general prescription, explained in Sec. IV D, we first calculated the one-step (p,α) cross sections for three choices of E_α: $E_\alpha=71$, 53, and 35 MeV, i.e., for $Q=(E_\alpha-E_p)=6$, -12, and -30 MeV. [In the following we shall refer to this triad of the Q values as (Q_1,Q_2,Q_3) or collectively as $\{Q\}$.] The cross sections for other E_α were then obtained by a logarithmic interpolation. For the two-step processes, accurate DWBA calculations were first performed for six pairs of Q values. The choices made were such that $(E_\alpha,E'_\alpha)=(71,71)$, (71,53), (71,35), (53,53), (53,35), and (35,35) MeV for the (p,α,α') processes, and that $(E'_p,E_\alpha)=(65,71)$, (65,53), (65,35), (47,53), (47,35), and (29,35) MeV for the (p,p',α) processes. [Note that in either case we have $(E_\alpha-E_p)=\{Q\}$ or $(E_\alpha-E'_p)=\{Q\}$.] The cross sections for other pairs of (E_α,E'_α) or of (E'_p,E_α) were obtained by using a two-dimensional logarithmic interpolation.

For the inelastic processes, either of protons or of α's, the first derivative of the optical potential, i.e., the LIFF of (4.7c), was used as the form factor. As for the spectroscopic density $\rho_l^{(ph)}(E_x)$, we used that of Ref. 9, i.e., that which is given by (4.9), rather than that of Ref. 6, i.e., that which is given by (4.4b) combined with (4.7a). The use of the former, which includes the ground-state correlation, i.e., the collectivity effect, makes $\rho_l^{(ph)}(E_x)$ larger, particularly for lower E_x.

The construction of the form factor pertaining to the triton pickup was made as follows. As shown above, all three processes involve the triad $\{Q\}$ for this pickup step. We constructed the triton c.m. wave function as bound in a Woods-Saxon potential, with the binding energy corresponding to the particular choice from the $\{Q\}$. We further chose things so that this wave function had $\{(n,\bar{l})\}=(3,4)$, (2,4), and (1,4), respectively, for $Q=Q_1$, Q_2, and Q_3, where n and $\bar{l}$ are, respectively, the node number and the orbital angular momentum. Note that these $(n,\bar{l})$'s have the total (oscillator) quantum number $N=2n+\bar{l}=10$, 8, and 6, which are the representative values of the sum of quantum numbers of the three nucleons to be picked up for each choice from the $\{Q\}$. Finally, we used (4.10b) for the spectroscopic density $\rho_{lj}^{(3h)}(E_x)$ to be used for the (p,α) step.

The results obtained in this way are compared with experiment[30] in Fig. 7. The agreement with the experimental angular distribution, seen in the left-hand column of Fig. 7, is about the same quality as seen in a similar comparison made in Fig. 6.

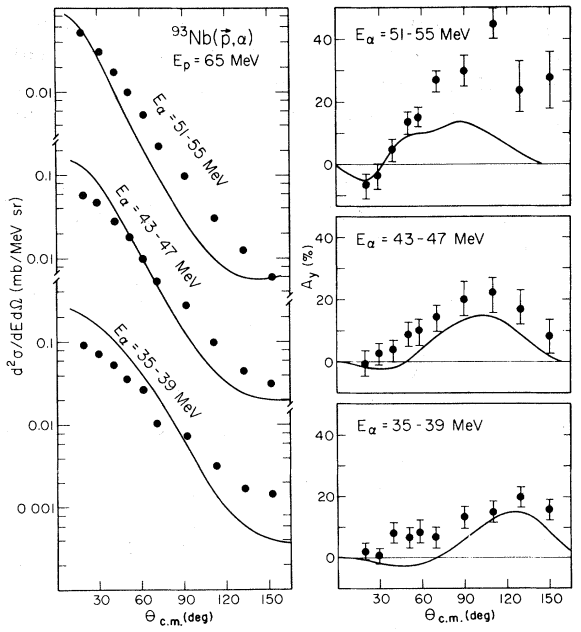

FIG. 7. Comparison of the calculated (p,α) cross sections and analyzing powers with experiment of Ref. 30. The solid lines include both one-step (p,α), two-step (p,α,α'), and (p,p',α) contributions.

To obtain this fit, we used for the D_0 factor (of the zero-range DWBA theory) a value of 141 MeV fm$^{3/2}$. To the extent that this D_0 value is accepted, the fit shown in Fig. 7 includes that of the magnitude.

In the right-hand column of Fig. 7, we compare the calculated A_y with experiment, and it is seen that a very good agreement was achieved for the two lower E_α bins. In the highest E_α bin, however, the theory underpredicts experiment by a factor of about 2 for $\theta > 60°$, possibly indicating that for such high E_α, the calculation we have performed was an oversimplification. To perform a less simplified calculation is not difficult, however, once we concentrate on a high E_α region. A high E_α means a low E_x, which results in a very limited number of elementary states. To treat these elementary states individually is not so difficult, and the above discrepancy may hopefully be removed in this way.

The A_y's in all the E_α bins are characterized by a large bump in the $\theta = 70° - 160°$ region. Our calculation shows that this bump is mainly due to the (p,α,α') process. As seen in Fig. 8, which shows for the $E_\alpha = 43 - 47$ MeV bin the separate contributions of the above three processes, the (p,α,α') is by far dominant over the other two, and this process also has a large bump in the large angle region. It is thus seen that the experimental bump is indeed accounted for largely by the (p,α,α') process.

Figures 7 and 8 should have been the same as Figs. 1 and 2 of Ref. 14, because the same data were analyzed in (essentially) the same way. Actually they differ, because we discovered an error in our computer program after Ref. 14 was published, and what we gave in Figs. 7 and 8 are results of our reanalysis made after the above error was corrected. In Ref. 14, we remarked that the dominant process was (p,p',α). This should be replaced by the correct statement made above that the dominant process is (p,α,α') instead.

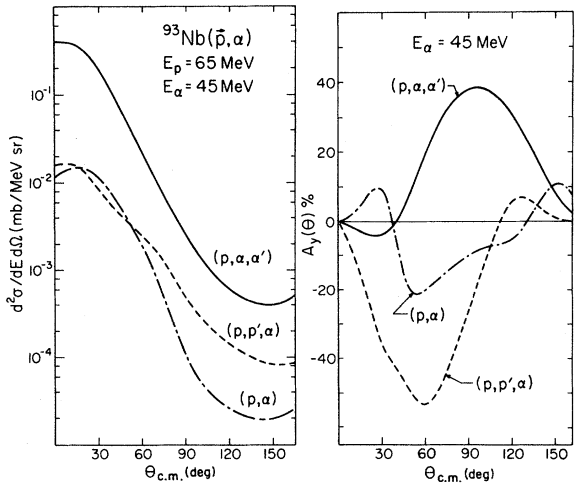

FIG. 8. Decomposition of contributions from one- and two-step processes to the cross sections and the analyzing powers given in Fig. 7.

VI. COMMENTS ON RELATED THEORIES

A theory which was used extensively in the past, in order to fit continuum spectra, is the so-called preequilibrium decay (PED) model, first proposed by Griffin[39] and then developed by Blann.[40] Although this early model was successful in fitting data that showed deviation from the predictions of the equilibrium decay model, it had a shortcoming in that it could predict only angle integrated spectra.

In order to remove this trouble, Manzouranis, Weidenmüller, and Agassi (MWA) (Ref. 41) reformulated the PED model, and arrived at an expression for the continuum cross section, which may be written, somewhat schematically, as

$$\sigma(E;\theta) = \sum_{n=1}^{N} \int \rho_n(E_x)\sigma_n(E,E';\theta,\theta')\,dE'd\theta' \,. \tag{6.1}$$

In (6.1), the nth term is the nth step contribution to $\sigma(E;\theta)$, and involves a $2(n-1)$-fold integral over the intermediate energies and angles, which are written symbolically as E' and θ', respectively. The level density $\rho_n(E_x)$ of (6.1) is evaluated in terms of the *exciton model,* and is not very much different from our ρ, introduced in Sec. IV. Thus, the MWA theory appears rather close to ours.

There is, however, an important difference. While we calculate the elementary cross sections based on the DR theory, applied to a *finite* nucleus, MWA calculates σ_n in (6.1) based on a cascadelike theory, applied to an *infinite* nuclear matter. Perhaps because of this, the series in (6.1) appears rather slowly convergent, making $\sigma(E;\theta)$ depend sensitively upon the choice of N. In other words, MWA theory involves N as a parameter which is rather *ad hoc.*

When N is chosen appropriately, the MWA theory fits experimental spectra rather nicely, particularly at the lower energy end. For the higher energy end, however, the theory often underestimates the experimental cross sections,[42] which, we believe, is again due to the use of the infinite matter. As is well known, the DR theory which we

use emphasizes the peripheral region. It allows for a large fraction of the projectiles to leave the interaction region, only after a very small number of steps, resulting in sufficiently large cross sections for high energy components. When an infinite matter is assumed, on the other hand, there remains little chance for the higher energy components to survive. Another possible problem with this approach is that, when the outgoing particle is, e.g., α, its preformation probability would have to be assumed.

The intranuclear cascade (INC) model, developed by the Oak Ridge and Brookhaven groups,[43,44] was of course applied to finite nuclei, and was very successful in fitting data taken for protons with a few hundred MeV incident energy. When used to analyze data for protons with a few tens of MeV energy, however, a difficulty was encountered; the predicted cross sections fell off too fast as the angle was increased.[45] The INC assumes a straight (classical) path between nucleon-nucleon collisions. Thus the diffraction, which is taken into account automatically when the MSDR theory is used, is not included in the INC calculations. This is likely the origin of the above mentioned trouble.

Several authors[18,46] had used DR theory to fit continuum spectra before or after we started our own MSDR work.[6–14] Nevertheless, their calculations were limited to one-step processes, thus restricting the applications to data with comparatively low energy projectiles, or to the high-energy end of the spectra when dealing with data with relatively high energy projectiles.

In a more recent paper, Feshback, Kerman, and Koonin (FKK) (Ref. 47) presented a MSDR theory for continuum which is very similar to ours. Since their presentation is not as explicit as ours, it is somewhat difficult to compare these two theories in every detail. It will, nevertheless, be safe to understand that both theories derive the one-step cross sections in the same way. As for the two-step cross sections, we may understand that the FKK formula is also represented by our formula given by (4.5a), if our (4.5b) is replaced by

$$d\sigma^{(2)}_{J_1J_2}(E_b,E_c;\theta_b)/d\Omega_b=(k_c^2/16\pi^2)\int[d\sigma^{(1)}_{J_2}(E_b,E_c;\theta_b\Omega_c)/d\Omega_b][d\sigma^{(1)}_{J_1}(E_c,E_a;\Omega_c 0)/d\Omega_c]d\Omega_c\ . \tag{6.2}$$

In (6.2), the one-step cross section $d\sigma^{(1)}/d\Omega$ has an explicit dependence on $Q_c(=\hat{k}_c)$, which is the direction of the momentum, $\vec{k}_c$, of the projectile in the intermediate channel c. The magnitude of $\vec{k}_c$ is, of course, related to E_c by $E_c=\hbar^2k_c^2/2\mu_c$.

Before obtaining (6.2), FKK arrived at an expression for the two-step amplitude which is very much like ours given, e.g., by (3.17b) together with (3.15b). They made several approximations, however, which we have not, and this resulted in a much simpler expression given by (6.2). We shall now show what approximations are made in FKK.

In order to simplify the presentation, we shall restrict ourselves to the case with $s=0$. With this restriction, the distorted waves in the k representation, as used by FKK, rather than in the partial wave representation, as we have used above, are given as

$$\chi^{(+)}(\vec{k},\vec{r})=(4\pi/kr)\sum_l i^l\chi_l(r)\sum_m Y_{lm}(\hat{r})Y^*_{lm}(\hat{k})\ , \tag{6.3a}$$

$$\tilde{\chi}^{(-)}(\vec{k},\vec{r})=(4\pi/kr)\sum_l i^l S_l^{-1}\chi_l\sum_m Y_{lm}(\hat{r})Y^*_{lm}(\hat{k})\ . \tag{6.3b}$$

We also have to have $\tilde{\chi}^{(+)}(\vec{k},\vec{r})$ and $\chi^{(-)}(\vec{k},\vec{r})$, which are outgoing and incoming wave solutions of (3.6a), in which D_a is replaced by D_a^* (an optical model with a source term). They are normalized as

$$\int\tilde{\chi}^{(+)*}(\vec{k},\vec{r})\chi^{(+)}(\vec{k}',\vec{r})d\vec{r}=\int\tilde{\chi}^{(-)*}(\vec{k},\vec{r})\chi^{(-)}(\vec{k}',\vec{r})d\vec{r}=(2\pi)^3\delta(\vec{k}-\vec{k}')\ , \tag{6.4}$$

and also have a property that

$$\int\tilde{\chi}^{(+)*}(\vec{k},\vec{r})\tilde{\chi}^{(-)}(\vec{k}',\vec{r})d\vec{r}=(2\pi)^3k^{-2}\delta(k-k')\sum_l S_l^{-1}\sum_m Y_{lm}(\hat{k})Y^*_{lm}(\hat{k})\ . \tag{6.5}$$

In (6.5), S_l is the elastic scattering S-matrix element. In the event that $S_l=1$ for all l, the rhs of (6.5) becomes the same as that of (6.4).

By using (6.3), it is not difficult to show that we obtain

$$d\sigma^{(2)}_{J_1J_2}(E_b,E_c;\theta_b)/d\Omega_b = \mu_b\mu_a(2\pi\hbar^2)^{-2}(k_b/k_a) \times \sum_{m_1m_2} |\langle\chi^{(-)}(\vec{k}_b)|v_{l_2m_2}|\chi^{(+)}(\vec{k}'_c)\rangle[E'_c-E_c-i\epsilon]^{-1}, \langle\tilde{\chi}^{(+)}(\vec{k}'_c)|v_{l_1m_1}|\chi^{(+)}\vec{k}_a)\rangle d\vec{k}'_c/(2\pi)^3|^2 . \quad (6.6)$$

Here $v_{lm}(\vec{r})=f(r)Y_{lm}(\hat{r})$. The two-step cross section given by (6.6) is still exactly the same as that given in Sec. III. Note that the matrix element in (6.6) that describes the first-step transition is of the form $\langle\tilde{\chi}^{(+)}|v|\chi^{(+)}\rangle$, rather than $\langle\chi^{(-)}|v|\chi^{(+)}\rangle$, which one encounters with, e.g., the one-step DWBA amplitude. The appearance of the $\langle\tilde{\chi}^{(+)}|v|\chi^{(+)}\rangle$ element is due to the biorthogonality nature of the distorted waves, as exemplified by (6.4).

We shall now list three approximations made by FKK: (i) to ignore the biorthogonality, that is, to replace $\langle\vec{\chi}^{(+)}|v|\chi^{(+)}\rangle$ by $\langle\tilde{\chi}^{(+)}|\tilde{\chi}^{(-)}\rangle \times\langle\chi^{(-)}|v|\chi^{(+)}\rangle$ (which is still exact), and then to set $\langle\tilde{\chi}^{(+)}|\tilde{\chi}^{(-)}\rangle=1$. Since $\langle\tilde{\chi}^{(+)}|\tilde{\chi}^{(-)}\rangle$ is nothing but the lhs of (6.5), this approximation is the same as to assume $S_l=1$ for all l, as discussed following (6.5). (ii) To replace $[E'_c-E_c-i\epsilon]^{-1}$ factor in (6.6) by $i\pi\delta(E'_c-E_c)$, i.e., to make the pole approximation of the Green's function. (In FKK, the use of the pole approximation was done in a slightly different manner, but the results are the same.) Note that the $d\vec{k}'_c$ integral in (6.6) is now replaced by a $d\hat{k}'_c$ integral. (iii) To insert a $\delta(\hat{k}'_c-\hat{k}''_c)$ factor in the $d\hat{k}'_c\,d\hat{k}''_c$ integral that results when the (absolute) square is taken in the summand of (6.6). If all these three approximations are made, (6.6) reduces to (6.2).

All these approximations are rather drastic, at least from the point of view of using the MSDR theory in fitting data of discrete state transition.[5] It may, nevertheless, happen that the errors introduced by the use of these approximations are washed out when continuum cross sections are considered, a point of view which appears to have been taken by FKK. In any case, we feel it desirable to carry out detailed numerical investigations to assess the validity of the FKK approximations.

Among the three approximations, (i) tends to *underestimate* the cross sections (sometimes rather drastically). This is because $|S_l|\ll 1$ and thus $|S_l^{-1}|\gg 1$, for some important l values. When approximation (i) is made, $|S_l^{-1}|$ is set equal to 1, making the amplitude pertaining to this l much smaller than it is when evaluated more accurately. Approximation (ii) may also tend to *underestimate* the cross section, although it would vary from one case to another. Compared with the above two, (iii) seems to tend to overestimate the cross section; we have experienced this in a few sample calculations which produced two sets of results, with and without this approximation.

Under favorable situations it may happen that the above opposing tendencies work together, so that the continuum cross sections predicted with the FKK approximations agree rather closely with those that are calculated with a less approximate method, like ours. Under unfavorable situations, however, it may not be impossible that two results differ significantly. We are currently investigating how these two compare under various conditions.

Very recently, Bonetti *et al.*[48] applied the FKK theory for the analyses of several (p,n) continuum data.[32] Contrary to our earlier work,[8] which was limited to the ^{208}Pb(p,n) reaction with $E_p=45$ MeV (see Sec. V B), they analyzed more cases with several different targets, and with E_p ranging from 25 to 45 MeV. It is seen[48] that good fits to data were obtained, in general, although there are seen also cases in which fits are not necessarily very good.

Limiting to the ^{208}Pb(p,n) reaction with $E_p=45$ MeV, for which two types of calculations are available (ours and FKK's), we may say that the predictions of the two theories are rather similar. For one thing, both theories fit data with about the same quality. For another, both show that it is necessary and (almost) sufficient to consider one- and two-step contributions.

There are, nevertheless, subtle differences. The relative significance of the two-step contributions is somewhat larger in the calculation of Bonetti *et al.* than it is in ours. This means that in their calculations, e.g., the contributions of the three-step contributions of the three-step processes are not entirely negligible. (We have not estimated the three-step contributions with our method.) We do not know, at this moment, whether this difference originated from their use[48] of the FKK approximations, as we mentioned above, or is due to their use of the strengths of the p-n and p-p (and n-n) interactions, which were taken as adjustable (within relatively narrow ranges). Further investigations do seem necessary before we can answer these questions unequivocally.

VII. CONCLUDING REMARKS

We have explained first why we believed that the MSDR theory could be used to analyze continuum data, and then presented formulation of the calculations to be performed. In the few examples that we showed, it was seen that the fits to data, achieved with our method, were in general very good.

All the examples we considered were reactions induced by protons with $E_p = 65$ MeV or less, and we showed that it was sufficient to consider one- and two-step contributions. One may naturally ask whether the three-step contributions were indeed negligible, or more generally, whether our expansion does converge.

From the forms of Eqs. (4.4a) and (4.5a), one may easily guess that the three-step cross section is written, somewhat schematically, as

$$d\sigma^{(3)}/dE\,d\Omega = \sum\sum\sum \int\int \rho(E_x)\rho(E_x')\rho(E_x'')d\sigma^{(3);\mathrm{DW}}/d\Omega \ . \tag{7.1}$$

The threefold summation is over the transferred angular momenta in three steps, while the twofold integrals are over the two intermediate energies. The third order DWBA cross section $d\sigma^{(3);\mathrm{DW}}/d\Omega$ may be very small, but its smallness may be compensated for by the presence of the threefold summation. The question is whether or not the ρ^3 factor in the integrand can be sufficiently large.

To make the matter explicit, let us keep in mind a (p,p') reaction with $E_p = 60$ MeV, and consider the excitation of the target by 30 MeV. It is then easy to see that the contribution of the ρ^3 factor is the largest when this total excitation energy is shared equally by the three steps, i.e., when $E_x = E_x' = E_x'' = 10$ MeV. With this low E_x, however, each ρ, and hence the ρ^3 factor in the integrand, remain rather small; and it eventually makes $d\sigma^{(3)}/dE\,d\Omega$ much smaller than the corresponding one- and two-step cross sections.

As the above example shows, there is always an upper limit of the number of steps beyond which we do not need to consider, once the upper limit of the excitation (of the residual nucleus) to be considered is fixed. For a given incident energy, there is a natural upper limit to this excitation energy. Therefore, there is also a natural upper limit of the number of steps to be considered. In this sense, our expansion is guaranteed to converge.

We have remarked above that the two-step calculations were already fairly time consuming, and thus one might wonder what we could do, when it indeed becomes necessary to calculate the three-step cross sections. We have experienced in the two-step calculations, however, that the cross sections, in particular the angular distributions, were very weakly dependent on the (pair of) transferred angular momenta, unless these angular momenta were both very small. This situation would be more so the case with the three-step transitions. This means that we would not need to perform calculations for all the triads of transferred angular momenta. We may calculate accurately the cross sections for a limited number of selected triads. The cross sections for other triads may be obtained easily and accurately by using, e.g., an interpolation.

When projectiles other than the nucleon were used, there occurs a process, the breakup process, which very often dominates the continuum cross sections. We shall not go into this subject in the present paper, however. We have, along with a few other authors, discussed this subject in a few recent publications, and the reader is referred to these papers.[49]

This work was supported in part by the U. S. Department of Energy, and by the Deutsche Forschungsgemeinschaft.

[1]N. Austern, *Direct Nuclear Reaction Theories* (Wiley, New York, 1970); G. R. Satchler, Nucl. Phys. 55, 1 (1964).

[2]T. Tamura, Phys. Rep. 14C, 61 (1974); T. Tamura, T. Udagawa, and M. C. Mermaz, *ibid.* 65, 345 (1980).

[3]R. J. Ascuito and N. K. Glendenning, Phys. Rev. 181, 1936 (1969); T. Udagawa, Phys. Rev. C 9, 270 (1974).

[4]T. Ohmura, B. Imanishi, M. Ichimura, and M. Kawai, Prog. Theory. Phys. (Kyoto) 41, 391 (1969).

[5]W. R. Coker, T. Udagawa, and H. H. Wolter, Phys. Rev. C 7, 1154 (1973).

[6]T. Tamura, T. Udagawa, D. H. Feng, and K. K. Kan, Phys. Lett. 66B, 109 (1977).

[7]T. Tamura and T. Udagawa, Phys. Lett. 71B, 273 (1977).

[8]T. Tamura and T. Udagawa, in Proceedings of the Symposium on Neutron Cross Sections from 10 to 40 MeV, edited by M. R. Bhat and S. Pearlstein, Brookhaven National Laboratory Report, BNL-NCS-50681, 1977, p. 533.

[9]T. Tamura and T. Udagawa, Phys. Lett. 78B, 189 (1978).

[10]T. Tamura, in *Proceedings of the International Workshop on Reaction Models for Continuum Spectra of Light Particles,* edited by J. Ernst (University of Bonn, Bonn, Germany, 1978), p. 1.

[11]T. Udagawa and T. Tamura, in *Giant Multipole Resonances,* edited by F. E. Bertrand (Harwood-Academic, New York, 1980), p. 467.

[12]H. Lenske, T. Tamura, and T. Udagawa, in *Polarization Phenomena in Nuclear Physics—1980 (Fifth International Symposium, Sante Fe),* Proceedings of the Fifth International Symposium on Polarization Phenomena in Nuclear Physics, AIP Conf. Proc. No. 69, edited by G. G. Ohlsen *et al.* (AIP, New York, 1980), p. 565.

[13]T. Tamura and T. Udagawa, in *Highly Excited States in Nuclear Reactions,* edited by H. Ikegami and M. Muraoka (Osaka University, Osaka, 1980), p. 33.

[14]T. Tamura, H. Lenske, and T. Udagawa, Phys. Rev. C 23, 2769 (1981).

[15]T. Udagawa and T. Tamura, in *Continuum Spectra in Heavy Ion Reactions,* edited by T. Tamura, J. B. Natowitz, and D. H. Youngblood (Harwood-Academic, New York, 1980), p. 155; T. Udagawa and T. Tamura, Lecture Notes at RCNP (Research Center for Nuclear Physics)—Kikuchi Summer School, edited by T. Yamazaki *et al.* (Osaka University, Osaka, 1980), p. 171.

[16]T. Tamura, Rev. Mod. Phys. 37, 679 (1965).

[17]A. Bohr and B. R. Mottelson, *Nuclear Structure* (Benjamin, London, 1975), Vol. II.

[18]G. F. Bertsch and S. F. Tsai, Phys. Rep. 18C, 125 (1975); S. F. Tsai and G. F. Bertsch, Phys. Rev. C 11, 1634 (1975).

[19]K. F. Liu and G. E. Brown, Nucl. Phys. A265, 385 (1976).

[20]S. Krewald and J. Speth, Phys. Lett. 52B, 295 (1974); J. Speth, E. Werner, and W. Wild, Phys. Rep. 33C, 129 (1977).

[21]H. Lenske, T. Tamura, and T. Udagawa (unpublished).

[22]M. Ichimura, A. Arima, E. C. Halbert, and T. Terasawa, Nucl. Phys. A204, 225 (1973).

[23]F. E. Bertrand and R. W. Peelle, Phys. Rev. C 8, 1045 (1973); Oak Ridge National Laboratory Reports ORNL-4455, 1969 and ORNL-4638, 1971.

[24]G. R. Satchler, Nucl. Phys. A195, 1 (1972); Phys. Rep. 14C, 97 (1974).

[25]S. F. Tsai and G. F. Bertsch, Phys. Lett. 73B, 247 (1978).

[26]F. Petrovich *et al.*, Phys. Rev. Lett. 22, 895 (1969); E. C. Halbert and G. R. Satchler, Nucl. Phys. A233, 265 (1974).

[27]H. D. Holmgren, C. C. Chang, R. W. Koontz, and J. R. Wu, in Proceedings of the International Conference on Nuclear Reaction Mechanism, Varena, Italy, 1979.

[28]A. K. Kerman and K. W. McVoy, Ann. Phys. (N.Y.) 122, 197 (1979).

[29]T. Udagawa and T. Tamura, Phys. Rev. Lett. 45, 1311 (1980).

[30]H. Sakai *et al.,* Phys. Rev. Lett. 44, 1193 (1980); Nucl. Phys. A344, 41 (1980); H. Sakai, private communication.

[31]J. J. H. Menet, E. E. Gross, J. J. Malanify, and A. Zucker, Phys. Rev. C 4, 1114 (1971).

[32]R. R. Doering, D. M. Patterson, and A. Galonsky, Phys. Rev. C 12, 378 (1975).

[33]F. G. Perey, Phys. Rev. 131, 745 (1963).

[34]F. E. Bertrand and R. W. Peelle, Oak Ridge National Laboratory Repot ORNL-4469, 1970.

[35]O. Dragun, A. M. Ferrero, and A. Pacheco, Nucl. Phys. A369, 149 (1981).

[36]E. Gadioli, I. Iori, M. Molho, and L. Zetta, Instituto Nazionale di Física Nucleare Report INFN/BE-73/5, 1973; A. M. Ferrero, I. Iori, N. Molho, and L. Zetta, Instituto Nazionale di Física Nucleare Report INFN/BE-78/6, 1978.

[37]Z. Lewandowski *et al.,* Phys. Lett. 95B, 207 (1980); R. Wagner, private communication.

[38]J. R. Sheperd, W. R. Zimmermann, and J. J. Kraushaar, Nucl. Phys. A257, 189 (1977).

[39]J. J. Griffin, Phys. Rev. Lett. 17, 478 (1966); Phys. Lett. 24B, 5 (1967).

[40]M. Blann, Phys. Rev. Lett. 21, 1357 (1971); Annu. Rev. Nucl. Sci. 25, 123 (1975); see also E. Gadioli, Nucleonika 21, 385 (1976).

[41]G. Mantzouranis, H. A. Weidenmüller, and D. Agassi, Z. Phys. A 276, 145 (1976).

[42]G. Mantzouranis, Phys. Rev. C 14, 2018 (1976).

[43]K. Chen, G. Friedlander, G. D. Harp, and J. M. Miller, Phys. Rev. C 4, 2234 (1971); H. W. Bertini, *ibid.* 6, 631 (1972).

[44]H. W. Bertini, G. D. Harp, and F. E. Bertrand, Phys. Rev. C 10, 2472 (1974).

[45]A. Galonsky, R. R. Doering, D. M. Patterson, and H. W. Bertini, Phys. Rev. C 14, 748 (1976).

[46]R. Reif, Acta Phys. Slovaca 25, 208 (1975); H. Lenske and G. Baur, Annual Report Institut für Kernphysik Kernforschungsanlage, Jülich, 1977, p. 109; M. B. Lewis, Phys. Rev. C 11, 145 (1975); T. Ishimatsu, M. Niwano, N. Kawamura, H. Ohmura, and T. Awaya, Nucl. Phys. A336, 205 (1980); I. Kumabe, K. Fukuda, and M. Matoba, Phys. Lett. 92B, 15 (1980); J. Ernst, J. Bisplinghott, T. Mayer-Kuckuk, J. Pampus, J. Rama-Rao, G. Baur, H. Lenske, F. Rösel, and D. Trautmann, Proceedings of the International Conference on Nuclear Reaction Mechanisms, Varena, Italy, 1977.

[47]H. Feshbach, A. K. Kerman, and S. E. Koonin, Ann. Phys. (N.Y.) 125, 429 (1980).

[48]R. Bonetti, M. Camnasio, L. Colli Milazzo, and P. E. Hodgson, Phys. Rev. C 24, 71 (1981).

[49]G. Baur and D. Trautmann, Phys. Rep. 25C, 293 (1976); T. Udagawa and T. Tamura, Phys. Rev. C 21, 1271 (1980); T. Udagawa, T. Tamura, T. Shimoda, H. Frölich, M. Ishihara, and K. Nagatani, *ibid.* 20, 1949 (1979).